The impact of extracellular matrix on the precision medicine utility of pancreatic cancer patient-derived organoids

Jan C. Lumibao[1], Shira R. Okhovat[1], Kristina Peck[1], Kathryn Lande[1], Jingjing Zou[2*], Dannielle D. Engle[1*]

[1]Salk Institute for Biological Studies, [2]University of California San Diego

Keywords: organoids, PDAC, pharmacotyping, precision medicine, basement membrane extract

*Co-corresponding authors

Corresponding author:
Dannielle D. Engle, Ph.D.
Salk Institute for Biological Studies
10010 N. Torrey Pines Rd.
La Jolla, CA 92037
Phone: (858) 453-4100 X1312
E-mail: engle@salk.edu

Conflict of interest: The authors have declared that no conflict of interest exists

Word count: 4364
Figures: 11
Tables: 2

Abstract

The use of patient-derived organoids (PDOs) to characterize therapeutic sensitivity and resistance (pharmacotyping) is a promising precision medicine approach with potential to inform clinical decisions that is now being tested in several large multi-institutional clinical trials. PDOs are cultivated in extracellular matrix from basement membrane extracts (BMEs) that are most commonly acquired commercially. Each clinical site utilizes distinct BME lots and may be restricted due to the availability of commercial BME sources. However, the impact of different sources and lots of BMEs on organoid drug response is unknown. Here, we tested the impact of BME source and lot on proliferation, chemotherapy and targeted therapy drug response, and gene expression in mouse and human pancreatic ductal adenocarcinoma (PDA). Both human and mouse organoids displayed increased proliferation in Matrigel compared to Cultrex (RnD) and UltiMatrix (RnD). However, we observed no substantial impact on organoid drug response when cultured in Matrigel, Cultrex, or UltiMatrix. We also did not observe major shifts in gene expression across the different BME sources, and PDOs maintained their Classical or Basal-like designation. Overall, we find that BME source (Matrigel, Cultrex, UltiMatrix) does not significantly nor substantially shift PDO dose-response curves and drug testing results.

Introduction

Pancreatic ductal adenocarcinoma (PDA) is projected to soon become the second leading cause of cancer death (*1*). Surgical resection remains the only curative option. However, most patients are ineligible due to metastasis at the time of diagnosis (*2*). Standard-of-care chemotherapeutic regimens include gemcitabine/nab-paclitaxel and FOLFIRINOX, which demonstrate median survival times of 8.5 and 11.1 months, respectively. Recently, the American Cancer Society reported the 5-year relative survival rate for patients with pancreatic cancer to be 11%. However, as the incidence of PDA continues to rise (*1*), strategies to increase survival are imperative. Further, as heterogeneity in tumor biology and treatment response continues to be revealed, personalized medicine approaches are becoming increasingly necessary.

The use of patient-derived organoids (PDOs) has the potential to revolutionize the care for patients with PDA (*3*). PDOs are 3D cultures in defined conditions that support propagation of normal, premalignant, and neoplastic cells from primary tissue (*4, 5*). Organoid technology has emerged as a promising avenue for precision medicine (*6*). The ability to derive PDA PDOs from surgical resections, rapid autopsies, and endoscopic ultrasound guided fine needle aspiration (EUS-FNA) biopsies allows for a broad sampling of the PDA patient population to encompass inter- and intrapatient tumor heterogeneity (*5*). Importantly, PDA PDOs mirror patient tumor genetics as well as treatment response, situating them as a promising tool for more personalized medicine efforts to identify alternative treatment strategies for chemorefractory tumors (*5, 7-9*).

As the use of organoids has expanded and become more accessible, variations in culture conditions have been introduced to optimize PDA PDO generation and growth. A number of studies have delineated the impact of media composition on organoid phenotype, transcriptome, and drug response (*10, 11*). Commercial products to support organoid studies have become more widespread, including a wide variety of basement membrane extracts (BME), which serve as 3D scaffolds. The use of fully synthetic and defined hydrogels to support organoids of colon, bile duct, and mammary gland origin have been recently described (*12-15*). However, BMEs derived from

Engelbreth-Holm-Swarm (EHS) murine sarcomas, most notably Matrigel (Corning), but also including products such as Cultrex and UltiMatrix (RnD), remain the most widely used (*13*). EHS-tumor-derived BMEs contain heterogenous mixtures of extracellular matrix proteins, primarily laminins, collagen IV, entactin, and perlecan, as well as tumor-derived proteins and growth factors, which contribute to batch-to-batch variability (*12, 13*). Regardless, these BMEs have historically served as the scaffold for organoid culture. However, the impact of different EHS-tumor-derived BMEs on organoid growth, chemosensitivity, and global gene expression remains unclear. Importantly, previous reports have demonstrated the clinical utility and relevance of PDA PDO pharmacotyping utilizing Matrigel (*5, 7, 9*). These studies and others have prompted the design of clinical trials targeting the use of organoid-guided chemotherapy. However, due to the CoVID-19 pandemic, severe supply chain issues have limited BME availability. These issues range from complete inability to secure the same commercial source of BME or dramatic reduction of available BME within the same lot. The impact of the commercial source and lot of BME on drug response and prognostic gene expression programs has not been explored, yet is critical for the deployment of PDO clinical trials.

Here, we report the impact of BME on PDA organoid growth, response to standard-of-care chemotherapy as well as targeted therapy, and gene expression patterns. While we find that BME source has a significant and substantial impact on organoid growth, drug response and gene expression remain consistent across lot and commercial source. Results from this study provide insights into selecting BME for organoid culture and, specifically, experiments to characterize PDO sensitivity and resistance to chemotherapies and targeted therapies which may assist in guiding clinical decisions.

53 **Results**

54 *BME impacts mouse and human organoid growth*

55 To investigate the influence of BME on organoid growth and dose-response phenotype,
56 human and mouse PDA organoids were cultivated in Matrigel 04 (lot #1062004) and then plated
57 for drug testing in either Matrigel 04, Matrigel 01 (lot #0287001), Cultrex 83 (lot #1564183), Cultrex
58 87 (lot #1586187), or UltiMatrix 96 (lot #1637796). Organoids were allowed to reform and then
59 subjected to pharmacotyping against PDA standard-of-care chemotherapies: gemcitabine,
60 paclitaxel, SN-38 (active metabolite of irinotecan), oxaliplatin, and 5-fluorouracil (5-FU), as well
61 as the targeted small molecule trametinib (third generation MEKi) (**Supplementary Figure 1**).
62 Human PDOs included hF24 (Stage IV, EUS-FNA), hM1F (Stage IV, lung metastasis, RAP), and
63 hT1 (Stage IIB, resection), and mouse organoids included mT69A [*LSL-Kras*$^{G12D/+}$*;LSL-*
64 *Trp53*$^{R172H/+}$*;Pdx-1-Cre* (KPC) local pancreatic metastasis] and mT69B (KPC primary pancreatic
65 tumor) (**Supplementary Table 1A-B**).

66 To compare proliferation of the organoid cultures in different BMEs, we measured
67 intracellular ATP levels (Cell Titer Glo) after 3 (mouse organoids) to 5 (human PDOs) days.
68 Human PDOs and mouse organoids exhibited reduced growth in Cultrex and UltiMatrix compared
69 to Matrigel (**Figure 1A-B, Supplementary Figure 2**). Mouse organoid proliferation did not recover
70 even after multiple passages in Cultrex, suggesting that this growth deficit is not due to a lack of
71 adaptation period (data not shown). In most experimental replicates across mouse and human
72 organoids, there was no difference in proliferation between Matrigel lots. In 1 out of 3 experiments,
73 there was a small but significant decrease in proliferation in hM1F (9% decrease) and hF24 (9%
74 decrease) PDOs in Matrigel 01 (**Supplementary Figure 2A-B**). Similarly, 1 out of 2 experiments
75 demonstrated a significant decrease in hT1 proliferation in Matrigel 01 (24% decrease)
76 (**Supplementary Figure 2C**). Mouse organoid mT69B consistently exhibited no significant
77 differences in intracellular ATP levels between Matrigel lots (n=4/4 experiments), while mT69A
78 exhibited small but significant changes between Matrigel lots in 2 out of 4 experiments

79 (**Supplementary Figure 2D-E**). In nearly all hPDO experiments, there was a significant, and
80 sometimes substantial (e.g., 27% in Cultrex 83 relative to Matrigel 04, $p < 0.0001$), reduction in
81 growth when cultured in either lot of Cultrex or UltiMatrix compared to Matrigel 04 (**Figure 1A,**
82 **Supplementary Figure 2A-B**). Mouse organoids exhibited more mixed results across
83 experimental repeats, but consistently (n=3/4 mT69A, n=4/4 mT69B) exhibited significant, and
84 sometimes substantial (e.g., 55% decrease in Ultimatrix 96 relative to Matrigel 04, $p < 0.0001$),
85 decreased growth in UltiMatrix 96 (**Figure 1B, Supplementary Figure 2D-E**). In the setting of
86 Cultrex, mouse organoid proliferation trended slower relative to Matrigel. mT69A and B grew
87 significantly slower in Cultrex 83 (A: n=2/4, B: 2/4) and 87 (A: n=3/4, B: 2/4), but in approximately
88 half of the experiments exhibited no significant difference relative to Matrigel 04. These data
89 collectively indicate that mouse and human organoids grow significantly more in Matrigel
90 compared to Cultrex or UltiMatrix.
91
92 *BME has minimal impact on drug response*
93 To investigate the influence of BME on drug response, we measured the dose-response
94 of both mouse and human organoids to standard of care chemotherapy as well as the third
95 generation MEK inhibitor trametinib. Specifically, we found that the dose-response curves for
96 gemcitabine, SN-38, and trametinib across all BMEs were largely overlapping in both hF24 and
97 hM1F in all 3 experimental repeats (**Figure 1C**, **Supplementary Figure 3A-B**) and largely
98 overlapping in hT1 in n=1/2, n=2/2, and n=1/2 experimental repeats, respectively
99 **(Supplementary Figure 3C**)**.** Dose-response curves across all BMEs for paclitaxel were also
100 largely overlapping in hM1F in n=3/3 experimental repeats (**Supplementary Figure 3B**) and in
101 hT1 in n=2/2 experimental repeats **(Supplementary Figure 3C**)**,** yet exhibited slight variability in
102 n=1/3 experimental repeats for hF24 (**Figure 1C, Supplementary Figure 3A).** Oxaliplatin also
103 displayed largely consistent dose-response curves regardless of BME in n=3/3 experimental
104 repeats for hF24, n=2/3 experimental repeats for hM1F, and n=2/2 experimental repeats for hT1

105 (**Figure 1C**, **Supplementary Figure 3A-C**). Additionally, 5-fluorouracil exhibited overlapping
106 dose-response curves in n=3/3 experimental repeats for hF24 (**Figure 3C**, **Supplementary**
107 **Figure 3A**) and n=2/3 experimental repeats for hM1F (**Supplementary Figure 3B**). However, we
108 observed more variability in dose-response curves for 5-fluorouracil in hT1 as a function of BME
109 in both experimental repeats conducted (**Supplementary Figure 3C**).

110 Mouse organoids were less sensitive to gemcitabine and SN-38 than their human
111 counterparts but exhibited no consistent or substantial shifts to their dose responses when
112 cultured in different BMEs (**Figure 1D**, **Supplementary Figure 3D-E**). Dose-response curves for
113 trametinib were also largely overlapping regardless of BME for both mT69A and mT69B, with
114 n=1/4 experimental replicates for both organoid lines displaying a shift to the right when organoids
115 were cultured in UltiMatrix 96 (**Supplementary Figure 3D-E**). We observed a similar
116 phenomenon for mouse organoids treated with paclitaxel (**Supplementary Figure 3D-E**).
117 Furthermore, we observed that both mT69A and mT69B were relatively resistant to oxaliplatin
118 and 5-fluorouracil, resulting in dose response curves that often did not achieve 50% cytotoxicity
119 (**Figure 1D, Supplementary Figure 3D-E**). Overall, these data demonstrate that choice of BME
120 does not induce significant shifts in dose-response curves for PDOs treated with standard-of-care
121 chemotherapies or trametinib, suggesting that either Matrigel, Cultrex, or UltiMatrix would be
122 appropriate for PDO pharmacotyping analyses.

123

124 *BME does not induce significant alterations in dose-response parameters*

125 To further compare differences in dose-response, we calculated IC50 concentrations and
126 area under the curve (AUC) for all dose-response curves whenever possible and plotted them
127 individually for each organoid-drug combination as a function of BME **(Figure 2**, **Supplementary**
128 **Figures 4-5**)**.** For all hPDOs, we observed no statistically significant alterations in mean IC50s
129 over experimental repeats calculated for any drug as a function of BME (**Figure 2A-B**,
130 **Supplementary Figure 4A**)**.** Similarly, mouse organoids exhibited no statistically significant shifts

131 in drug IC50, regardless of which BME organoids were plated in (**Supplementary Figure 4B-C**).
132 In line with these data, we rarely observed changes in drug dose-response curve AUCs across
133 BMEs. AUCs for hF24 treated with paclitaxel were slightly (1.28- to 1.3-fold) but statistically
134 significantly higher when pharmacotyping was conducted in Cultrex 83 or Cultrex 87 compared
135 to Matrigel 04 (**Figure 2C**). Similarly, calculated AUCs for hM1F treated with gemcitabine were
136 1.3-fold higher on average in Cultrex 83 compared to Matrigel 04 (**Figure 2D**). Lastly, AUCs for
137 mT69A treated with paclitaxel were increased in Ultimatrix 96 compared to Matrigel 04 (1.28-fold)
138 (**Supplementary Figure 5B**). In all other mouse and human drug-organoid combinations tested,
139 there were not significant differences in AUC across multiple experiments.

140 We next sought to analyze dose-response curve goodness-of-fit as a parameter of plating
141 consistency in each BME within and across experimental replicates. We employed a four-
142 parameter non-linear regression model to fit dose-response curves to cell viability data obtained
143 via CTG. Thus, standard deviation of the residuals (Sy.x) presented as the most appropriate
144 estimate of goodness-of-fit compared to other parameters such as R^2 or root mean square error.
145 In general, higher Sy.x values indicate larger deviations of data points from the fit regression
146 curve. Overall, we observed no statistically significant differences in Sy.x values for both human
147 and mouse organoids across BMEs and all drugs (**Figure 3, Supplementary Figure 6**). However,
148 for both human and mouse organoids, both lots of Matrigel exhibited more consistent Sy.x values
149 across experimental replicates compared to Cultrex or UltiMatrix, as evidenced by lower variance
150 in Sy.x values across experiments **(Figure 3**)**.**

151 In the context of hPDOs, Sy.x values for Cultrex 83 were relatively consistent across
152 experimental replicates, with relatively low absolute values (<10%) and low inter-experimental
153 variability (**Figure 3A**). The largest variations in Sy.x across experimental replicates in Cultrex
154 that we detected were hF24 treated with SN-38 and 5-FU, and hM1F treated with gemcitabine
155 and oxaliplatin (**Figure 3A-B**). Notably, absolute Sy.x values were larger on average for Cultrex
156 83 in hM1F treated with oxaliplatin (mean = 20.37%). Cultrex 87 performed consistently as well,

157 with the most statistical variance across experiments (ranging from 1.6 - 11.5%) observed in hF24
158 treated with gemcitabine (**Figure 3A**). UltiMatrix 96, relative to the other BMEs, exhibited higher
159 experimental variability in Sy.x values, with greater variance observed in hF24 treated with
160 gemcitabine (4.1 - 11%) and oxaliplatin (7.6 - 22.3%); and hM1F treated with gemcitabine (4.0 -
161 15.8%), paclitaxel (4.6 - 14.1%), oxaliplatin (7.5 - 26%), and trametinib (4.8 - 12.6%) (**Figure 3A-**
162 **B**). Matrigel 04 yielded consistent and relatively low Sy.x values (<10%) across all experimental
163 replicates, with the exception of hF24 treated with 5-fluorouracil (6.3 - 13.3%) (**Figure 3A**,
164 **Supplementary Figure 6**). Similarly, Matrigel 01 demonstrated low and consistent Sy.x values
165 across treatments, experimental replicates, and hPDOs tested, as evidenced by low standard
166 deviations and low Sy.x absolute values **(Figure 3A**, **Supplementary Figure 6**). Overall, these
167 results indicate better dose-response curve goodness-of-fit from experiment to experiment when
168 organoids are cultured in Matrigel.

169 For mouse organoids, similar trends were observed, albeit with higher absolute Sy.x
170 values across almost all conditions (range: 4.5 - 40.8%) (**Figure 3C-D**). In general, mouse
171 organoids are more sensitive to single cell dissociation protocols and have higher growth rates,
172 both of which contribute to increased variance and necessitate shorter pharmacotyping
173 experiment time courses (3 days for mouse organoids vs 5 days for hPDOs). Over the course of
174 4 experimental replicates, UltiMatrix 96 demonstrated a high degree of statistical variability in Sy.x
175 values relative to the other BMEs tested, notably for mT69A treated with paclitaxel (9.0 - 24.1%)
176 and oxaliplatin (13.5 - 23.9%), and mT69B treated with gemcitabine (8.81 - 19.8%) (**Figure 3C-**
177 **D**). Relative to the other BMEs tested, Cultrex lots also exhibited high levels of variability in Sy.x.
178 Cultrex 83 exhibited a high degree of variability for mT69A treated with 5-FU (7.7 - 22.7%) and
179 trametinib (5.9 - 14.7%), and mT69B treated with paclitaxel (6.3 - 17.1%) and SN-38 (7.3 - 40.8%)**.**
180 Similar variability across experimental replicates was observed for Cultrex 87 in mT69A treated
181 with oxaliplatin (11.7 - 26.8%) and 5-FU (12.2 - 30.5%), and mT69B treated with gemcitabine (6.9
182 - 19.4%), paclitaxel (7.9 - 23.6%), and trametinib (8.2 - 39.9%). Of note, across experimental

183 replicates, UltiMatrix 96 demonstrated exceptional consistency in Sy.x values for mT69B treated
184 with paclitaxel (10.7 - 10.9%). Both Matrigel 04 and Matrigel 01 again showed relatively consistent
185 Sy.x values in the mouse organoid context but were not exempt from biological and experimental
186 variance. Most notably, mT69A and mT69B are relatively resistant to oxaliplatin and 5-FU and
187 exhibited relatively high Sy.x absolute values (20-30%) compared to those observed from other
188 drug treatments (**Figure 3B**, **Supplementary Figure 3D-E**, **Supplementary Figure 4C-D**).
189 Overall, lot-to-lot variability was more pronounced for Cultrex compared to Matrigel for
190 both human and mouse organoids, and UltiMatrix presented with higher variability in Sy.x values
191 across experimental replicates. However, there were no statistically significant differences
192 detected in Sy.x values across BMEs within each organoid drug treatment. Collectively, these
193 data indicate that drug dose response curve fitting is stable across the BMEs tested.
194
195 *Gene expression and organoid subtype classification are not influenced by BME*
196 Although we did not observe substantial shifts in drug response as a function of BME lot
197 or type, alterations in intracellular signaling and cell state represented another potential variable
198 influenced by BME composition. Therefore, we also sought to determine whether different BME
199 sources induced changes in gene expression or PDA subtype classification (*16*). To this end,
200 mouse organoids (mT69A, mT69B, mT9) and human PDOs (hF24, hM1F, hT1) were cultured in
201 triplicate in each BME (Matrigel 04, Matrigel 01, Cultrex 83, Cultrex 87, and Ultimatrix 96) for three
202 days, and subjected to RNA-seq (**Figure S1A**). Analysis of differentially expressed genes
203 between BMEs revealed minimal organoid differential gene expression between both lots of
204 Matrigel for both human and mouse organoids (0-2 differentially expressed genes, 20 in hM1F)
205 (**Supplementary Figure 7A-B**). Similarly, there was minimal differential gene expression
206 observed in both human and mouse organoids between both lots of Cultrex (0-4 differentially
207 expressed genes) (**Supplementary FIgure 7A-B**). Interestingly, organoids derived from early
208 PDA disease stages tended to display greater numbers of differentially expressed genes between

209 Matrigel 04 and Cultrex 87 as well as UltiMatrix (**Supplementary Figure 7A-B**). For instance,
210 hT1 (Stage 2B) displayed 522 differentially expressed genes between Matrigel 04 and UltiMatrix,
211 whereas hF24 (Stage 4) and hM1F (Stage 4, lung metastasis) presented 0 (**Supplementary**
212 **Figure 7A**). Similarly, mT69B (KPC PDA primary tumor) displayed 90 differentially expressed
213 genes between Matrigel 04 and Cultrex 87, whereas mT69A (KPC PDA metastasis) presented
214 with 13 (**Supplementary Figure 7B**). These data suggest that organoids derived from later stage
215 malignant lesions display greater resilience to extracellular cues. Mutlivariate analysis of resultant
216 Z-scores of organoid normalized counts indicated that both mouse and human samples clustered
217 well based on organoid line (**Figure 4A**, **Supplementary Figure 7C-D**). However, we observed
218 no substantial or significant effect of BME on differential gene expression, and samples did not
219 cluster significantly based on BME (**Figure 4, Supplementary Figure 7C-D, F-G**). These results
220 indicate that BME does not remarkably alter PDO gene expression profiles.

221 Previous work defined molecular subtype of PDA with prognostic and therapeutic
222 resistance, with basal-like PDA exhibiting poorer prognoses and therapeutic resistance compared
223 to the classical subtype (*16*). Changes to molecular subtype would have major implications on
224 the predictive power of PDOs in precision medicine approaches. To determine whether BME
225 influenced hPDO subtype classification, we delineated significant changes to enrichment of basal-
226 like and classical differentially expressed genes. Pairwise comparisons of hallmark subtype gene
227 enrichment indicated no significant enrichment of either basal-like or classical genes between
228 Matrigel 04 and Matrigel 01 (**Supplementary Figure 7E**). Choice of BME did not influence
229 organoid molecular subtype classification or induce substantial alterations in enrichment of genes
230 associated with either the classical or basal-like subtype (**Figure 4A**). The classical subtype
231 organoid hF24 displayed significant enrichment of classical hallmark genes when cultured in
232 Cultrex 83 (p = 1.4E-7), Cultrex 87 (p = 0.00078), or UltiMatrix (p = 0.00078) compared to Matrigel
233 04 **(Supplementary Figure 7E**). Similarly, the basal-like organoid hM1F displayed upregulation
234 of basal-like hallmark genes when cultured in Cultrex 83 (p = 0.00042), Cultrex 87 (p = 1.4E-5),

235 or UltiMatrix (p = 0.0027) **(Supplementary Figure 7E).** Further analysis of individual genes
236 revealed that BME did not significantly alter hPDO expression levels of *KRAS*, *TP53*, or *CDKN2A*,
237 while there was a slight but statistically significant increase in *SMAD4* expression in hM1F
238 cultured in Matrigel 01 compared to Matrigel 04 (**Figure 4B**). Similarly, we observed slight yet
239 statistically significant increases in *ERBB3* in all three hPDOs cultured in Cultrex or UltiMatrix
240 (**Supplementary Figure 7H**). Expression of *EGFR* was increased in hT1 cultured in Cultrex 87
241 relative to Matrigel 04 (**Supplementary Figure 7H**). However, we did not observe any significant
242 changes in expression levels of other PDA relevant genes such as *MYC*, *GATA6*, *MAP2K1*,
243 *MAP2K2*, *SOX9*, *RB1*, *BRCA2*, and *ERBB2*, as well as genes related to drug resistance such as
244 *HNF1A* and *ABCB1* (**Supplementary Figure 7H**). Overall, these data indicate that choice of BME
245 does not significantly influence hPDO subtype classification or gene expression profiles.
246

247 **Discussion**

248 The predictive power of PDOs to mirror patient genetics, transcriptomics, and drug
249 response in retrospective studies prompted the onset of several clinical trials to use PDOs to
250 inform treatment decisions. However, previous studies demonstrated the plasticity of PDOs in
251 response to varying culture conditions and potential impact on PDO drug response (*10, 11*). With
252 multi-institutional clinical trials underway, the need to investigate factors that impact the
253 robustness of PDO genetics, transcriptomics, and drug testing is imperative. Basement
254 membrane extracts are central to most PDO efforts. Previous studies demonstrated variability in
255 protein composition, presence of xenogenic bioactive compounds, and scaffold stiffness between
256 batches. Despite this variability, commercially available BMEs remain critical and prevalent in
257 organoid efforts. Given the multi-year nature of PDO-related clinical trials, more than one lot of
258 BME will be required for the duration of these studies. In addition, limitations in availability due to
259 supply chain issues has necessitated that some efforts switch between alternate commercial

260 sources. However, the influence of BME source and lot on organoid response to drug treatment
261 was unknown.

262 To investigate the extent to which BME parameters impacts growth, drug response, and
263 transcriptomics, we compared various commercially available BMEs on previously established
264 mouse and human PDA organoids. We consistently observed a decrease in mouse and human
265 organoid proliferation when cultured in Cultrex or UltiMatrix compared to Matrigel. While this could
266 potentially arise from a lack of an adaptation period, multiple passages of mouse organoids in
267 Cultrex does not rescue their proliferative potential. Despite this growth deficit, we observed no
268 substantial shifts in drug response or gene expression as a function of BME source or lot. This
269 study made use of previously established organoids. Accordingly, the impact of BME on organoid
270 generation efficiency from primary tissue specimens has yet to be formally characterized and
271 would be of interest for future studies. For established organoids, Matrigel, Cultrex, or UltiMatrix
272 BMEs are all viable options for pharmacotyping experiments. Altogether, this work demonstrates
273 that precision medicine approaches using organoids are robust and that ongoing clinical trials are
274 unlikely to be affected by different lots or commercial sources of BME.

275

276 **Methods**

277 *Organoids and cell culture conditions*

278 Organoids used in this study were generated at Cold Spring Harbor Laboratory (*4, 5, 17*).
279 Human patient-derived and mouse organoids were cultured as described. In short, mouse
280 organoid media contained Advanced DMEM/F12, HEPES, Glutamax, Penicillin/Streptomycin,
281 EGF, FGF-10, Gastrin, A83-01, B27 supplement, *N*-acetylcysteine, nicotinamide, Noggin, and R-
282 spondin1. For human organoid culture, Wnt3a was also included in the media. Organoid
283 nomenclature is defined as: hT – human tumor obtained from resection; hF – human fine-needle
284 biopsy obtained by fine-needle aspiration or core biopsy; hM – human metastasis obtained from
285 direct resection of metastases following rapid autopsy or VATS resection; mT – murine tumor. All

286 organoid models were routinely tested for *Mycoplasma* at Salk Institute. Additional hPDO and
287 mouse organoid characteristics are available in **Table S1A** and **Table S1B**.
288
289 *Basement membrane extracts*
290 Both human and mouse organoids were maintained in Corning Matrigel Lot #1062004
291 during the growth and expansion phase. For pharmacotyping comparisons, organoids were plated
292 in either Corning Matrigel (Growth Factor Reduced, Phenol Red Free) Lot #1062004 (hereafter
293 denoted as Matrigel 04), Corning Matrigel (Growth Factor Reduced, Phenol Red Free) Lot
294 #0287001 (hereafter denoted as Matrigel 01), RnD Cultrex Reduced Growth Factor BME Lot
295 #1564183 (hereafter denoted as Cultrex 83), RnD Cultrex Reduced Growth Factor BME Lot
296 #1586187 (hereafter denoted as Cultrex 87), or Cultrex UltiMatrix Reduced Growth Factor BME
297 Lot #1637796 (hereafter denoted as UltiMatrix 96).
298
299 *Pharmacotyping of organoids*
300 Organoids were dissociated into single cells using a diluted solution of TrypLE Express
301 (Thermo Fisher). Equal numbers of single cells (1,500 viable cells per well) were plated in a 20
302 uL suspension of 10% BME in wells of black-walled, ultra-low attachment 384 well plates
303 (Corning). Twenty-four hours after plating, reformation of organoids was visually verified and
304 therapeutic compounds were applied. Chemotherapies were tested in triplicate 10-point dose-
305 response. Gemcitabine, paclitaxel, SN-38 (active metabolite of irinotecan), and trametinib ranged
306 from 0.5 nM – 5 μM; oxaliplatin and 5-fluorouracil ranged from 50 nM – 100 μM. Compounds were
307 dissolved in DMSO, and all treatments were normalized to 0.5% DMSO content. Mouse organoids
308 underwent treatment for 3 days, while human organoids underwent treatment for 5 days. After
309 treatment, cell viability was assessed using Cell Titer Glo (Promega) per manufacturer's
310 instructions on a Tecan Spark Cyto plate reader. A four-parameter log-logistic function with upper
311 limit equal to the mean of the lowest dose values was fit to the data (viability vs. dose) with

312 Graphpad Prism 9. The half maximal inhibitory concentration (IC50) values, area under the curve
313 (AUC), and standard deviation of the residuals (Sy.x) for each dose-response curve were
314 calculated using Graphpad Prism 9. Each pharmacotyping experiment was carried out at least
315 two times.
316
317 *RNA isolation*
318 For RNA-seq comparisons, organoids were maintained in Corning Matrigel Lot #1062004
319 (Matrigel 04) and then plated in either Corning Matrigel (Growth Factor Reduced, Phenol Red
320 Free) Lot #1062004 (Matrigel 04), Corning Matrigel (Growth Factor Reduced, Phenol Red Free)
321 Lot #0287001 (Matrigel 01), RnD Cultrex Reduced Growth Factor BME Lot #1564183 (Cultrex
322 83), RnD Cultrex Reduced Growth Factor BME Lot #1586187 (Cultrex 87), or Cultrex UltiMatrix
323 Reduced Growth Factor BME Lot #1637796 (Ultimatrix 96). Each BME condition was plated in
324 triplicate, and organoids were grown for 3 days before harvesting in TRIzol (Life Technologies)
325 and snap frozen. RNA was isolated using the RNeasy Mini Kit (Qiagen). RNA quality control was
326 performed for all samples using a Qubit Fluorometer (Life Technologies) and TapeStation (RIN
327 greater than 8.5) (Agilent) before RNA-seq analysis.
328
329 *RNA-seq analysis*
330 Library construction was conducted using the Truseq RNA library prep kit (Illumina) with
331 500 ng RNA input. Raw reads were trimmed with Trim Galore v0.4.4_dev
332 (https://www.bioinformatics.babraham.ac.uk/projects/trim_galore/) and quality-checked with
333 FastQC v0.11.8 (http://www.bioinformatics.babraham.ac.uk/projects/fastqc). Trimmed reads
334 were then aligned to the hg38 human reference genome with STAR aligner v2.5.3a (*18*), and
335 converted to gene counts with HOMER's analyzeRepeats.pl script (*19*).
336
337

338 *Differential gene expression analysis*

339 Gene counts where normalized and queried for differential expression using DESeq2
340 v1.30.0 (*20*). For each pairwise comparison, genes with fewer than 10 total raw counts across all
341 samples were discarded prior to normalization, and genes with an absolute log2foldchange > 1
342 and an FDR-corrected p-value ≤ 0.05 were pulled as significant.

343

344 *Functional enrichment*

345 Genes were queried for treatment-specific functional enrichment using over-
346 representation analysis (ORA) and gene set enrichment analysis (GSEA) in WebGestaltR v0.4.4
347 (*21*). Differentially expressed genes in each pairwise comparison were queried against the
348 biological process ontology with ORA, while pairwise GSEAs were used to query pathway gene
349 sets from KEGG (https://www.genome.jp/kegg/pathway.html), and MSigDB (http://www.gsea-
350 msigdb.org/gsea/msigdb/collections.jsp).

351

352 *Statistics*

353 A four-parameter log-logistic function with upper limit equal to the mean of the lowest dose
354 values was fit to the dose-response data (viability vs. dose) with Graphpad Prism 9. The half
355 maximal inhibitory concentration (IC50) values, area under the curve (AUC), and standard
356 deviation of the residuals (Sy.x) for each dose-response curve were calculated using Graphpad
357 Prism 9. Each pharmacotyping experiment was carried out for n = 2-4 experimental replicates.
358 Differences among means were analyzed using 1-way ANOVA with Dunnett's multiple
359 comparisons test. Outliers were determined using Grubbs' test $\alpha = 0.05$.

360

361

362

363

364 *Author contributions*

365 JL, SO, and KP designed and conducted the experiments and acquired and analyzed the
366 data. KL performed statistical analysis on RNA-seq data. JZ provided statistical analysis for dose-
367 response curve comparisons. JL and DE wrote the manuscript.

368

369 *Acknowledgements*

370 The authors are supported by National Institutes of Health, National Cancer Institute
371 R00CA024725 (Engle), P30DK120515 (Engle), T32CA009370 (Lumibao); the Pancreatic Cancer
372 Action Network 19-20-ENGL (Engle), American Association for Cancer Research and the
373 Lustgarten Foundation 21-20-67-ENGL (Engle), the University of California Tobacco-Related
374 Disease Research Program T31KT1898 (Engle), and Padres Pedal the Cause/C3 #PTC2020
375 (Engle). We are grateful to the Rose Hills Foundation, Mission Cure Capital, LLC, the Mark
376 Foundation for Cancer Research, and the Emerald Foundation, Inc. for supporting Dr. Engle.

377

378

379

380

381

382

383

384

385

386

387

388

389

390 **Figure legends**

391 **Figure 1. Basement membrane extract impacts proliferation of mouse and human**
392 **organoids but does not significantly shift dose-response curves.** (**A**) Proliferation of human
393 patient-derived organoids hF24 and hM1F cultured in Matrigel 04, Matrigel 01, Cultrex 83, Cultrex
394 87, or UltiMatrix 96 for 5 days as determined by Cell Titer Glo. Data represent mean ± SD.
395 Statistical significance was determined by 1-way ANOVA. ****$P \leq 0.0001$ vs. Matrigel 04. (**B**) Cell
396 Titer Glo of mouse organoids mT69A and mT69B cultured in Matrigel 04, Matrigel 01, Cultrex 83,
397 Cultrex 87, or UltiMatrix 96 for 3 days as determined by Cell Titer Glo. Data represent mean ±
398 SD. Statistical significance was determined by 1-way ANOVA. ****$P \leq 0.0001$ vs. Matrigel 04. (**C**)
399 Dose-response curves for hF24 treated with gemcitabine, paclitaxel, SN-38, oxaliplatin, 5-
400 fluorouracil (5-FU), and trametinib during culture in Matrigel 04, Matrigel 01, Cultrex 83, Cultrex
401 87, or UltiMatrix 96. Data represent mean ± SD of triplicate Cell Titer Glo values at each dose
402 fitted with a four-parameter log-logistic function with upper limit equal to the mean of the lowest
403 dose values. (**D**) Dose-response curves for mT69B treated with gemcitabine, paclitaxel, SN-38,
404 oxaliplatin, 5-fluorouracil (5-FU), and trametinib during culture in Matrigel 04, Matrigel 01, Cultrex
405 83, Cultrex 87, or UltiMatrix 96. Data represent mean ± SD of triplicate Cell Titer Glo values at
406 each dose fitted with a four-parameter log-logistic function with upper limit equal to the mean of
407 the lowest dose values.

408

409 **Figure 2. Basement membrane extracts exert minimal effects on drug IC50 and dose-**
410 **response AUC.** (**A-B**) Calculated IC50 values (M) for hF24 and hM1F treated with gemcitabine,
411 paclitaxel, SN-38, oxaliplatin, 5-fluorourical (5-FU), and trametinib during culture in Matrigel 04,
412 Matrigel 01, Cultrex 83, Cultrex 87, or UltiMatrix 96. Data represent mean ± SD of 3 experimental
413 replicates. (**C-D**) Calculated area under the curve (AUC) values for hF24 and hM1F treated with
414 gemcitabine, paclitaxel, SN-38, oxaliplatin, 5-FU, and trametinib during culture in Matrigel 04,
415 Matrigel 01, Cultrex 83, Cultrex 87, or UltiMatrix 96. Data represent mean ± SD of 3 experimental

416 replicates. Statistical significance was determined by 1-way ANOVA. *$P \leq 0.05$, ***$P \leq 0.001$ vs.
417 Matrigel 04.
418
419 **Figure 3. Dose-response curve goodness of fit is not significantly altered by basement**
420 **membrane extract.** (**A-B**) Standard deviation of the residuals (Sy.x) for hF24 and hM1F treated
421 with gemcitabine, paclitaxel, SN-38, oxaliplatin, 5-fluorourical (5-FU), and trametinib during
422 culture in Matrigel 04, Matrigel 01, Cultrex 83, Cultrex 87, or UltiMatrix 96. Data represent mean
423 ± SD of 3 experimental replicates. (**C-D**) Standard deviation of the residuals (Sy.x) for mT69A and
424 mT69B treated with gemcitabine, paclitaxel, SN-38, oxaliplatin, 5-fluorourical (5-FU), and
425 trametinib during culture in Matrigel 04, Matrigel 01, Cultrex 83, Cultrex 87, or UltiMatrix 96. Data
426 represent mean ± SD of 4 experimental replicates. Outliers were determined using Grubbs' test
427 $\alpha = 0.05$.
428
429 **FIgure 4. Human patient-derived organoid gene expression profiles are consistent across**
430 **basement membrane extract types.** (**A**) Heatmap of normalized counts of classical or basal-
431 like hallmark genes in hF24, hM1F, and hT1. Each organoid line was sequenced in triplicate after
432 culture for 3 days in Matrigel 04, Matrigel 01, Cultrex 83, Cultrex 87, or UltiMatrix 96. (B)
433 Normalized counts for hallmark PDA genes *KRAS, TP53, SMAD4,* and *CDKN2A*. Data represent
434 mean ± SD of 3 technical replicates. Statistical significance was determined by 1-way ANOVA.
435 **$P \leq 0.01$ vs. Matrigel 04.
436
437 **Supplementary Figure S1. Experimental outline.** Three biological replicates of human patient-
438 derived organoids and mouse organoids were selected based on primary sample type (resection
439 or endoscopic ultrasound-guided fine-needle aspiration) and disease stage. Each organoid line
440 was expanded to sufficient quantities for experimentation in Matrigel 04. Organoids were then
441 single-cell dissociated and either plated in triplicate in 6-well plates for RNA isolation and

442 subsequent RNA-seq, or plated for pharmacotyping in 5 384-well plates in Matrigel 04, Matrigel
443 01, Cultrex 83, Cultrex 87, or UltiMatrix 96. Organoids were allowed to recover overnight. Next,
444 organoids were treated with drugs and incubated for 5 days (human organoids) or 3 days (mouse
445 organoids), followed by Cell Titer Glo to assess organoid viability.
446
447 **Supplementary Figure S2. Proliferation of human and mouse organoids is not significantly**
448 **altered by basement membrane extract.** (**A**) Data for n = 3 experimental replicates of hF24
449 proliferation in Matrigel 04, Matrigel 01, Cultrex 83, Cultrex 87, or UltiMatrix 96. Data represent
450 mean ± SD. $^{**}P \leq 0.01$, $^{****}P \leq 0.0001$ vs. Matrigel 04. (**B**) Data for n = 3 experimental replicates
451 of hM1F proliferation in Matrigel 04, Matrigel 01, Cultrex 83, Cultrex 87, or UltiMatrix 96. Data
452 represent mean ± SD. $^{**}P \leq 0.01$, $^{****}P \leq 0.0001$ vs. Matrigel 04. (**C**) Data for n = 2 experimental
453 replicates of hT1 proliferation in Matrigel 04, Matrigel 01, Cultrex 83, Cultrex 87, or UltiMatrix 96.
454 Data represent mean ± SD. $^{****}P \leq 0.0001$ vs. Matrigel 04. (**D**) Data for n = 4 experimental
455 replicates of mT69A proliferation in Matrigel 04, Matrigel 01, Cultrex 83, Cultrex 87, or UltiMatrix
456 96. Data represent mean ± SD. $^{*}P \leq 0.05$, $^{**}P \leq 0.01$, $^{****}P \leq 0.0001$ vs. Matrigel 04. (**E**) Data for
457 n = 4 experimental replicates of mT69B proliferation in Matrigel 04, Matrigel 01, Cultrex 83, Cultrex
458 87, or UltiMatrix 96. Data represent mean ± SD. $^{**}P \leq 0.01$, $^{****}P \leq 0.0001$ vs. Matrigel 04.
459
460 **Supplementary Figure S3. Dose response curves are consistent regardless of basement**
461 **membrane extract used.** (**A**) Data for n = 3 experimental replicates of hF24 response to
462 gemcitabine, paclitaxel, SN-38, oxaliplatin, 5-fluorouracil (5-FU), and trametinib while cultured in
463 Matrigel 04, Matrigel 01, Cultrex 83, Cultrex 87, or UltiMatrix 96. Data represent mean ± SD of
464 triplicate Cell Titer Glo values at each dose fitted with a four-parameter log-logistic function with
465 upper limit equal to the mean of the lowest dose values. (**B**) Data for n = 3 experimental replicates
466 of hM1F response to gemcitabine, paclitaxel, SN-38, oxaliplatin, 5-fluorouracil (5-FU), and
467 trametinib while cultured in Matrigel 04, Matrigel 01, Cultrex 83, Cultrex 87, or UltiMatrix 96. Data

468 represent mean ± SD of triplicate Cell Titer Glo values at each dose fitted with a four-parameter
469 log-logistic function with upper limit equal to the mean of the lowest dose values. (**C**) Data for n =
470 2 experimental replicates of hT1 response to gemcitabine, paclitaxel, SN-38, oxaliplatin, 5-
471 fluorouracil (5-FU), and trametinib while cultured in Matrigel 04, Matrigel 01, Cultrex 83, Cultrex
472 87, or UltiMatrix 96. Data represent mean ± SD of triplicate Cell Titer Glo values at each dose
473 fitted with a four-parameter log-logistic function with upper limit equal to the mean of the lowest
474 dose values. (**D**) Data for n = 4 experimental replicates of mT69A response to gemcitabine,
475 paclitaxel, SN-38, oxaliplatin, 5-fluorouracil (5-FU), and trametinib while cultured in Matrigel 04,
476 Matrigel 01, Cultrex 83, Cultrex 87, or UltiMatrix 96. Data represent mean ± SD of triplicate Cell
477 Titer Glo values at each dose fitted with a four-parameter log-logistic function with upper limit
478 equal to the mean of the lowest dose values. (**E**) Data for n = 4 experimental replicates of mT69B
479 response to gemcitabine, paclitaxel, SN-38, oxaliplatin, 5-fluorouracil (5-FU), and trametinib while
480 cultured in Matrigel 04, Matrigel 01, Cultrex 83, Cultrex 87, or UltiMatrix 96. Data represent mean
481 ± SD of triplicate Cell Titer Glo values at each dose fitted with a four-parameter log-logistic function
482 with upper limit equal to the mean of the lowest dose values.
483
484 **Supplementary Figure S4. Calculated IC50 values remain consistent across basement**
485 **membrane extract culture conditions.** (**A**) Calculated IC50 values (M) for hT1 treated with
486 gemcitabine, paclitaxel, SN-38, oxaliplatin, 5-fluorourical (5-FU), and trametinib during culture in
487 Matrigel 04, Matrigel 01, Cultrex 83, Cultrex 87, or UltiMatrix 96. Data represent mean ± SD of 2
488 experimental replicates. (**B**) Calculated IC50 values (M) for mT69A treated with gemcitabine,
489 paclitaxel, SN-38, oxaliplatin, 5-fluorourical (5-FU), and trametinib during culture in Matrigel 04,
490 Matrigel 01, Cultrex 83, Cultrex 87, or UltiMatrix 96. Data represent mean ± SD of 4 experimental
491 replicates. (**C**) Calculated IC50 values (M) for mT69B treated with gemcitabine, paclitaxel, SN-
492 38, oxaliplatin, 5-fluorourical (5-FU), and trametinib during culture in Matrigel 04, Matrigel 01,

493 Cultrex 83, Cultrex 87, or UltiMatrix 96. Data represent mean ± SD of 4 experimental replicates.
494 Outliers were determined using Grubbs' test α = 0.05.
495
496 **Supplementary Figure S5. Calculated AUC values are consistent across basement**
497 **membrane extract culture conditions.** (**A**) Calculated area under the curve (AUC) values for
498 hT1 treated with gemcitabine, paclitaxel, SN-38, oxaliplatin, 5-FU, and trametinib during culture
499 in Matrigel 04, Matrigel 01, Cultrex 83, Cultrex 87, or UltiMatrix 96. Data represent mean ± SD of
500 2 experimental replicates. (**B**) Calculated area under the curve (AUC) values for mT69A treated
501 with gemcitabine, paclitaxel, SN-38, oxaliplatin, 5-FU, and trametinib during culture in Matrigel 04,
502 Matrigel 01, Cultrex 83, Cultrex 87, or UltiMatrix 96. Data represent mean ± SD of 4 experimental
503 replicates. Statistical significance was determined by 1-way ANOVA. *$P \leq 0.05$ vs. Matrigel 04.
504 (**C**) Calculated area under the curve (AUC) values for mT69B treated with gemcitabine, paclitaxel,
505 SN-38, oxaliplatin, 5-FU, and trametinib during culture in Matrigel 04, Matrigel 01, Cultrex 83,
506 Cultrex 87, or UltiMatrix 96. Data represent mean ± SD of 4 experimental replicates.
507
508 **Supplementary Figure S6. Standard deviation of the residuals does not statistically change**
509 **as a function of basement membrane extract used.** Standard deviation of the residuals (Sy.x)
510 for hT1 treated with gemcitabine, paclitaxel, SN-38, oxaliplatin, 5-fluorourical (5-FU), and
511 trametinib during culture in Matrigel 04, Matrigel 01, Cultrex 83, Cultrex 87, or UltiMatrix 96. Data
512 represent mean ± SD of 2 experimental replicates. Outliers were determined using Grubbs' test
513 α = 0.05.
514
515 **Supplementary Figure S7. Global gene expression profiles are consistent across**
516 **basement membrane extract conditions for both mouse and human organoids.** (**A**)
517 Differential gene expression among human patient-derived organoids cultured in Matrigel 04
518 (MG004), Matrigel 01 (MG001), Cultrex 83 (Cultrex 183), Cultrex 87 (Cultrex 187), or UltiMatrix

96 (Ultimatrix). Numbers represent total number of genes with an adjusted *P* value of differential expression ≤ 0.05 and an absolute log2(foldchange) > 1 for all pairwise comparisons of basement membrane extracts within individual organoid lines and within species. (**B**) Differential gene expression among mouse organoids cultured in Matrigel 04 (MG004), Matrigel 01 (MG001), Cultrex 83 (Cultrex 183), Cultrex 87 (Cultrex 187), or UltiMatrix 96 (Ultimatrix). Numbers represent total number of genes with an adjusted *P* value of differential expression ≤ 0.05 and an absolute log2(foldchange) > 1 for all pairwise comparisons of basement membrane extracts within individual organoid lines and within species. (**C**) Principal component analysis of human patient-derived organoid gene expression within species and individual organoid lines. (**D**) Principal component analysis of mouse organoid gene expression within species and individual organoid lines. (**E**) Heatmaps of basal-like or classical hallmark gene enrichment between basement membrane extract comparisons for all human patient-derived organoid lines (top row) and individual lines. Each square represents significance of enrichment in the differentially expressed genes between two basement membrane extracts. The differentially expressed genes in the basement membrane exract listed on the y-axis are queried for enrichment. Squares are labeled with *P* value. Black squares = ns. (**F**) Expression heatmap of all genes in human patient-derived organoids cultured in different basement membrane extracts. Z-scores of normalized counts. (**G**) Expression heatmap of all genes in mouse organoids cultured in different basement membrane extracts. Z-scores of normalized counts. (**H**) Normalized counts for select genes of interest in hF24, hM1F, and hT1 cultured in different basement membrane extracts. Data represent mean ± SD of 3 technical replicates. *$P \leq 0.05$, **$P \leq 0.01$ vs. Matrigel 04.

545 **References**

546 1. R. Abbassi, H. Algül, Palliative chemotherapy in pancreatic cancer-treatment sequences.
547 *Transl Gastroenterol Hepatol* **4**, 56 (2019).

548 2. J. Kleeff *et al.*, Pancreatic cancer. *Nat Rev Dis Primers* **2**, 16022 (2016).

549 3. T. T. Seppälä *et al.*, Patient-derived Organoid Pharmacotyping is a Clinically Tractable
550 Strategy for Precision Medicine in Pancreatic Cancer. *Ann Surg* **272**, 427-435 (2020).

551 4. S. F. Boj *et al.*, Organoid models of human and mouse ductal pancreatic cancer. *Cell* **160**,
552 324-338 (2015).

553 5. H. Tiriac *et al.*, Organoid Profiling Identifies Common Responders to Chemotherapy in
554 Pancreatic Cancer. *Cancer Discov* **8**, 1112-1129 (2018).

555 6. E. Driehuis, K. Kretzschmar, H. Clevers, Establishment of patient-derived cancer
556 organoids for drug-screening applications. *Nat Protoc* **15**, 3380-3409 (2020).

557 7. E. Driehuis *et al.*, Pancreatic cancer organoids recapitulate disease and allow
558 personalized drug screening. *Proceedings of the National Academy of Sciences of the*
559 *United States of America* **116**, 26580-26590 (2019).

560 8. S. Hou *et al.*, Advanced Development of Primary Pancreatic Organoid Tumor Models for
561 High-Throughput Phenotypic Drug Screening. *SLAS Discov* **23**, 574-584 (2018).

562 9. T. T. Seppälä *et al.*, Precision Medicine in Pancreatic Cancer: Patient-Derived Organoid
563 Pharmacotyping Is a Predictive Biomarker of Clinical Treatment Response. *Clinical cancer*
564 *research : an official journal of the American Association for Cancer Research* **28**, 3296-
565 3307 (2022).

566 10. S. Raghavan *et al.*, Microenvironment drives cell state, plasticity, and drug response in
567 pancreatic cancer. *Cell* **184**, 6119-6137.e6126 (2021).

568 11. T. L. Hogenson *et al.*, Culture media composition influences patient-derived organoid
569 ability to predict therapeutic responses in gastrointestinal cancers. *JCI Insight* **7**, (2022).

570 12. N. Broguiere *et al.*, Growth of Epithelial Organoids in a Defined Hydrogel. *Adv Mater* **30**,
571 e1801621 (2018).
572 13. E. A. Aisenbrey, W. L. Murphy, Synthetic alternatives to Matrigel. *Nat Rev Mater* **5**, 539-
573 551 (2020).
574 14. S. Randriamanantsoa *et al.*, Spatiotemporal dynamics of self-organized branching in
575 pancreas-derived organoids. *Nat Commun* **13**, 5219 (2022).
576 15. S. Khan, H. Tiriac, Synthetic scaffold for pancreatic organoids. *Nat Mater* **21**, 9-11 (2022).
577 16. R. A. Moffitt *et al.*, Virtual microdissection identifies distinct tumor- and stroma-specific
578 subtypes of pancreatic ductal adenocarcinoma. *Nat Genet* **47**, 1168-1178 (2015).
579 17. J. S. Roe *et al.*, Enhancer Reprogramming Promotes Pancreatic Cancer Metastasis. *Cell*
580 **170**, 875-888.e820 (2017).
581 18. A. Dobin *et al.*, STAR: ultrafast universal RNA-seq aligner. *Bioinformatics* **29**, 15-21
582 (2013).
583 19. S. Heinz *et al.*, Simple combinations of lineage-determining transcription factors prime cis-
584 regulatory elements required for macrophage and B cell identities. *Mol Cell* **38**, 576-589
585 (2010).
586 20. M. I. Love, W. Huber, S. Anders, Moderated estimation of fold change and dispersion for
587 RNA-seq data with DESeq2. *Genome Biol* **15**, 550 (2014).
588 21. Y. Liao, J. Wang, E. J. Jaehnig, Z. Shi, B. Zhang, WebGestalt 2019: gene set analysis
589 toolkit with revamped UIs and APIs. *Nucleic Acids Res* **47**, W199-w205 (2019).
590

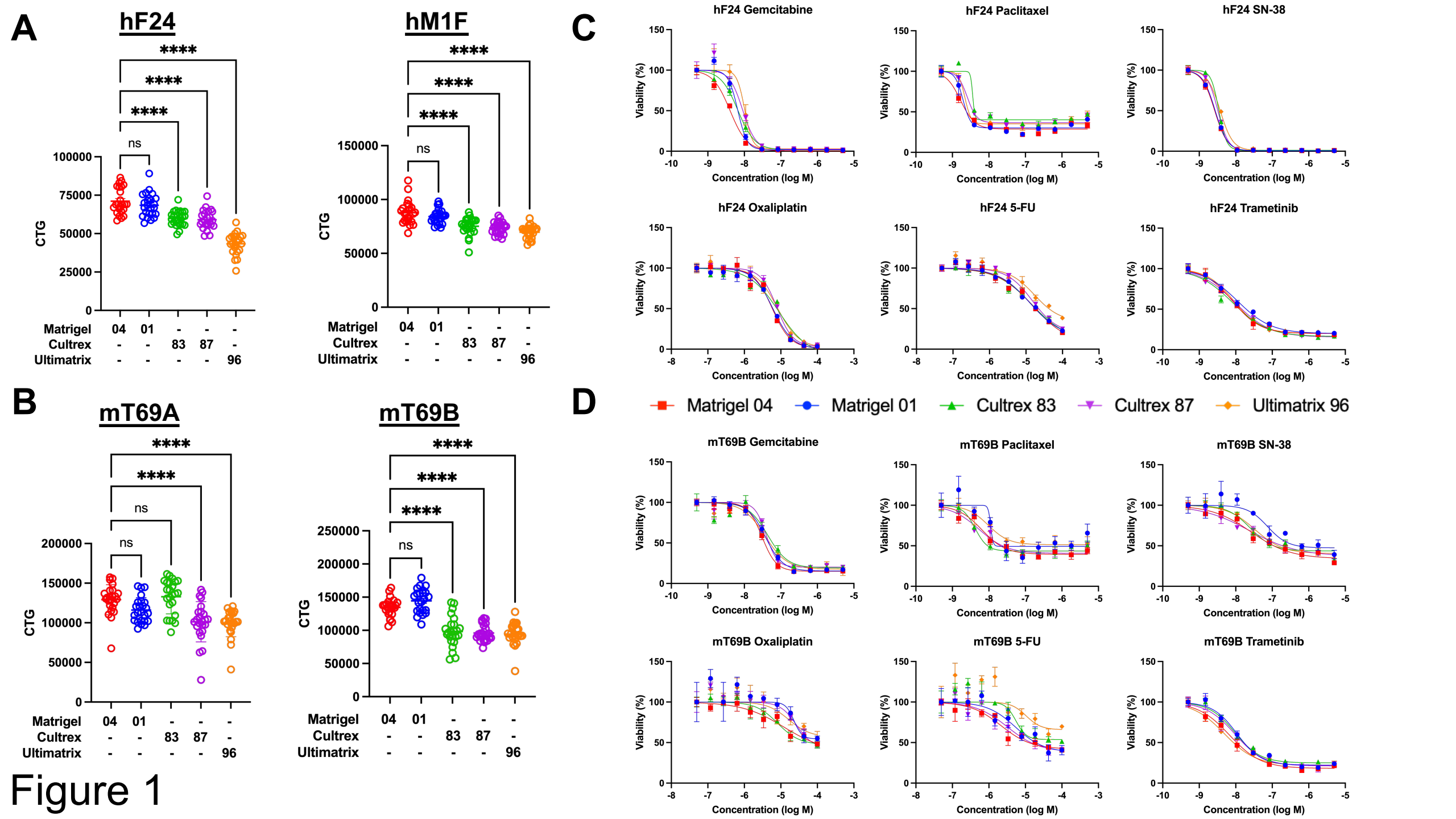
A
hF24
hM1F
B
mT69A
mT69B
C
hF24 Gemcitabine
hF24 Paclitaxel
hF24 SN-38
hF24 Oxaliplatin
hF24 5-FU
hF24 Trametinib
D
mT69B Gemcitabine
mT69B Paclitaxel
mT69B SN-38
mT69B Oxaliplatin
mT69B 5-FU
mT69B Trametinib
CTG
Viability (%)
Concentration (log M)
ns
****
Matrigel
Cultrex
Ultimatrix
04
01
83
87
96
Matrigel 04
Matrigel 01
Cultrex 83
Cultrex 87
Ultimatrix 96

Figure 1

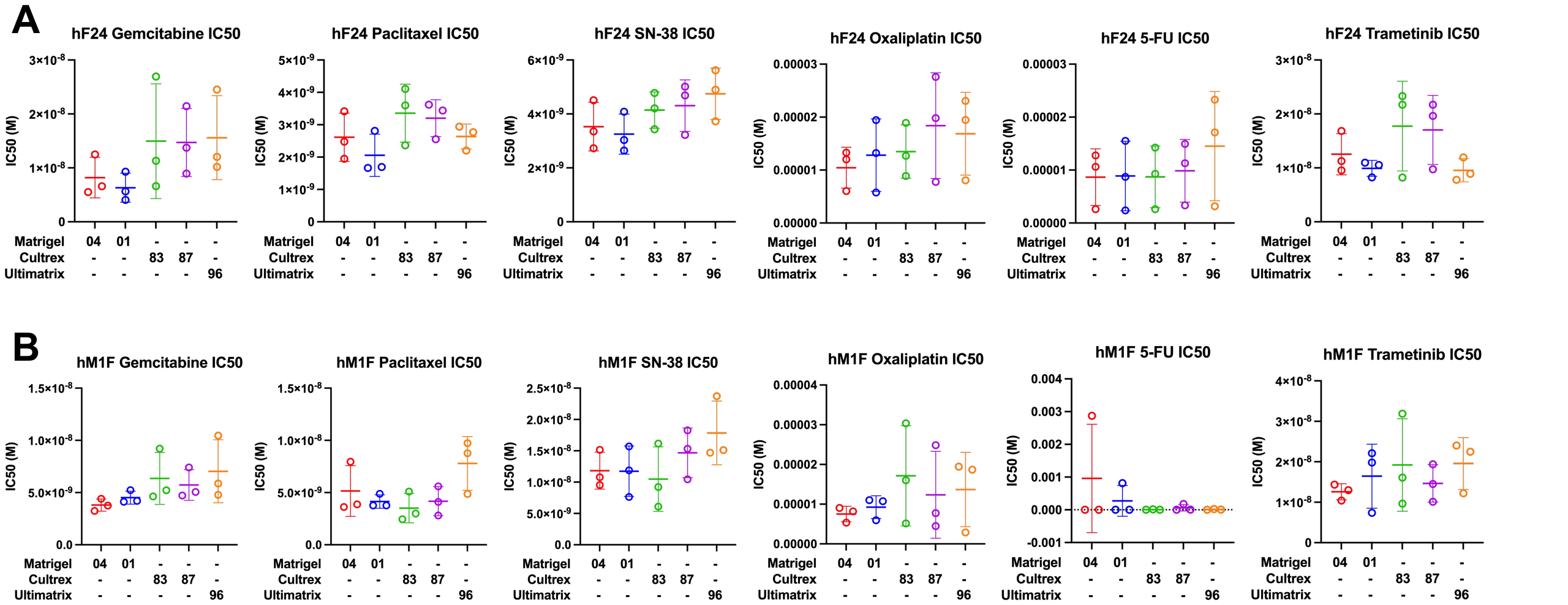
A
hF24 Gemcitabine IC50
hF24 Paclitaxel IC50
hF24 SN-38 IC50
hF24 Oxaliplatin IC50
hF24 5-FU IC50
hF24 Trametinib IC50
B
hM1F Gemcitabine IC50
hM1F Paclitaxel IC50
hM1F SN-38 IC50
hM1F Oxaliplatin IC50
hM1F 5-FU IC50
hM1F Trametinib IC50
IC50 (M)
Matrigel 04 01 - - -
Cultrex - - 83 87 -
Ultimatrix - - - - 96

Figure 2A-B

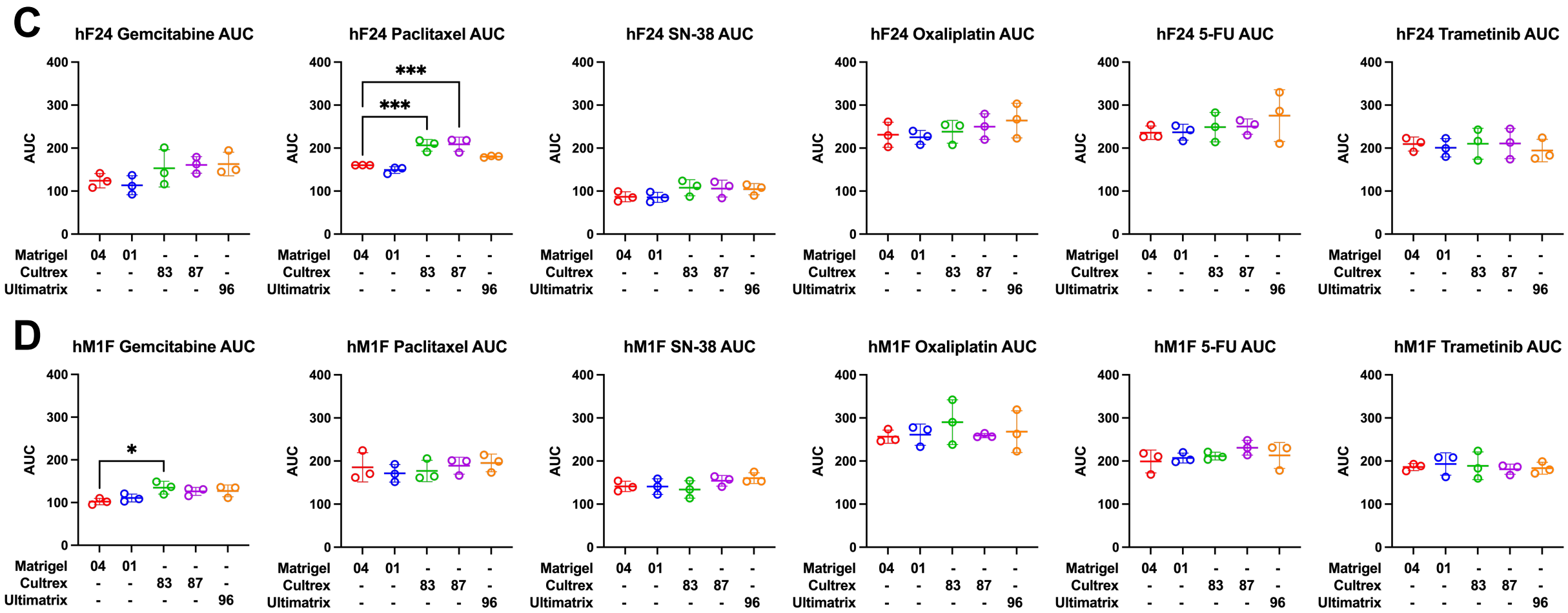
C
hF24 Gemcitabine AUC
hF24 Paclitaxel AUC
hF24 SN-38 AUC
hF24 Oxaliplatin AUC
hF24 5-FU AUC
hF24 Trametinib AUC
D
hM1F Gemcitabine AUC
hM1F Paclitaxel AUC
hM1F SN-38 AUC
hM1F Oxaliplatin AUC
hM1F 5-FU AUC
hM1F Trametinib AUC
AUC
0
100
200
300
400
***
*
Matrigel 04 01 - - -
Cultrex - - 83 87 -
Ultimatrix - - - - 96

Figure 2C-D

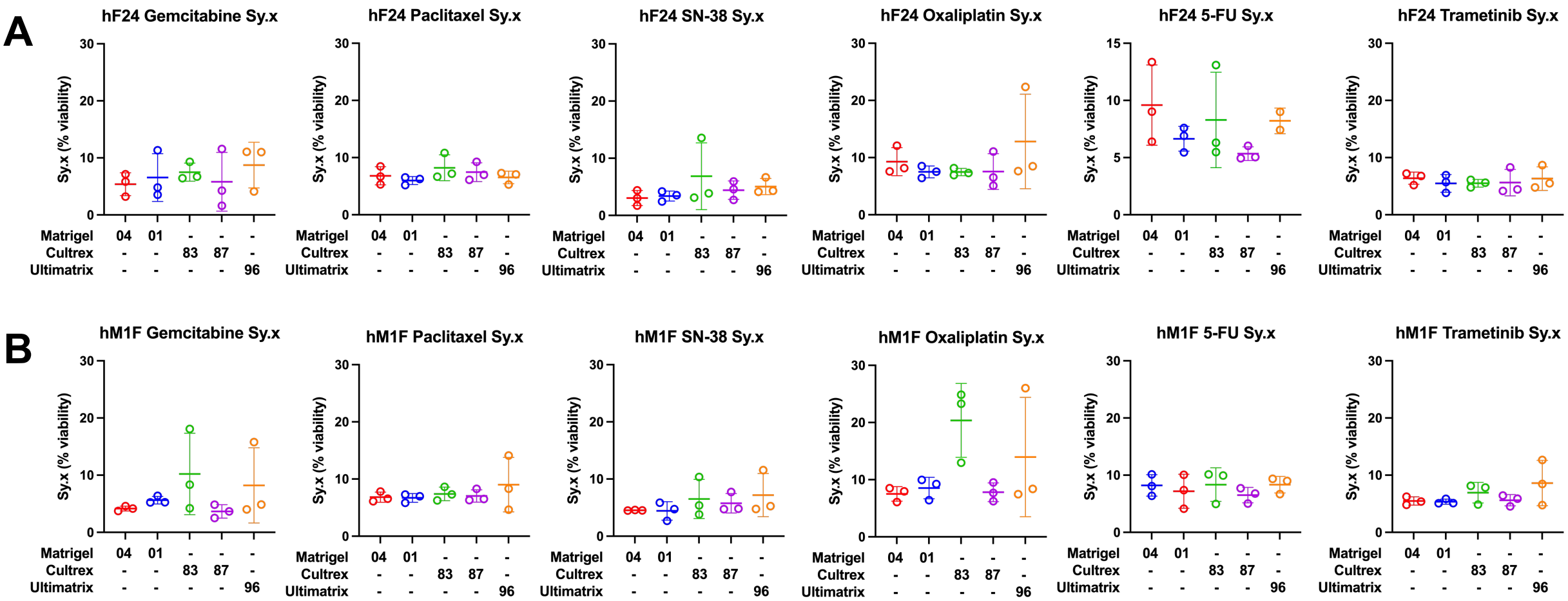
A
hF24 Gemcitabine Sy.x
hF24 Paclitaxel Sy.x
hF24 SN-38 Sy.x
hF24 Oxaliplatin Sy.x
hF24 5-FU Sy.x
hF24 Trametinib Sy.x
B
hM1F Gemcitabine Sy.x
hM1F Paclitaxel Sy.x
hM1F SN-38 Sy.x
hM1F Oxaliplatin Sy.x
hM1F 5-FU Sy.x
hM1F Trametinib Sy.x
Sy.x (% viability)
Matrigel 04 01 - - -
Cultrex - - 83 87 -
Ultimatrix - - - - 96

Figure 3A-B

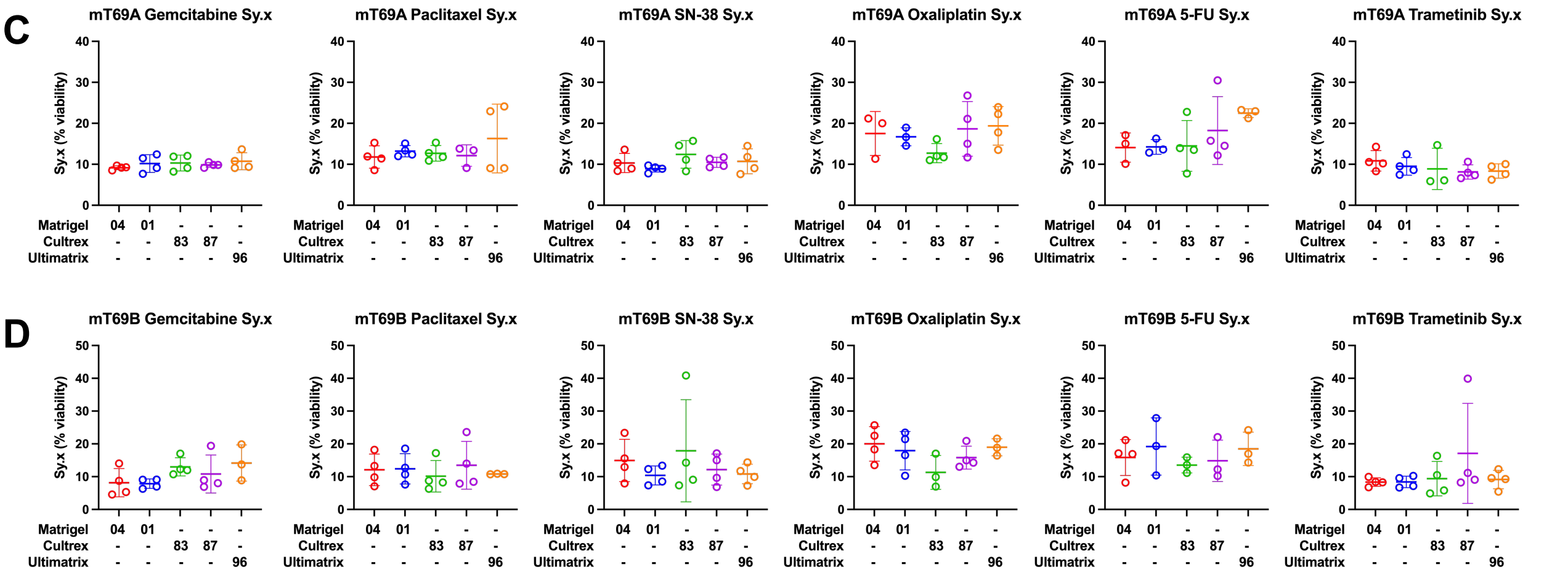
C
mT69A Gemcitabine Sy.x
mT69A Paclitaxel Sy.x
mT69A SN-38 Sy.x
mT69A Oxaliplatin Sy.x
mT69A 5-FU Sy.x
mT69A Trametinib Sy.x
D
mT69B Gemcitabine Sy.x
mT69B Paclitaxel Sy.x
mT69B SN-38 Sy.x
mT69B Oxaliplatin Sy.x
mT69B 5-FU Sy.x
mT69B Trametinib Sy.x
Sy.x (% viability)
Matrigel 04 01 - - -
Cultrex - - 83 87 -
Ultimatrix - - - - 96

Figure 3C-D

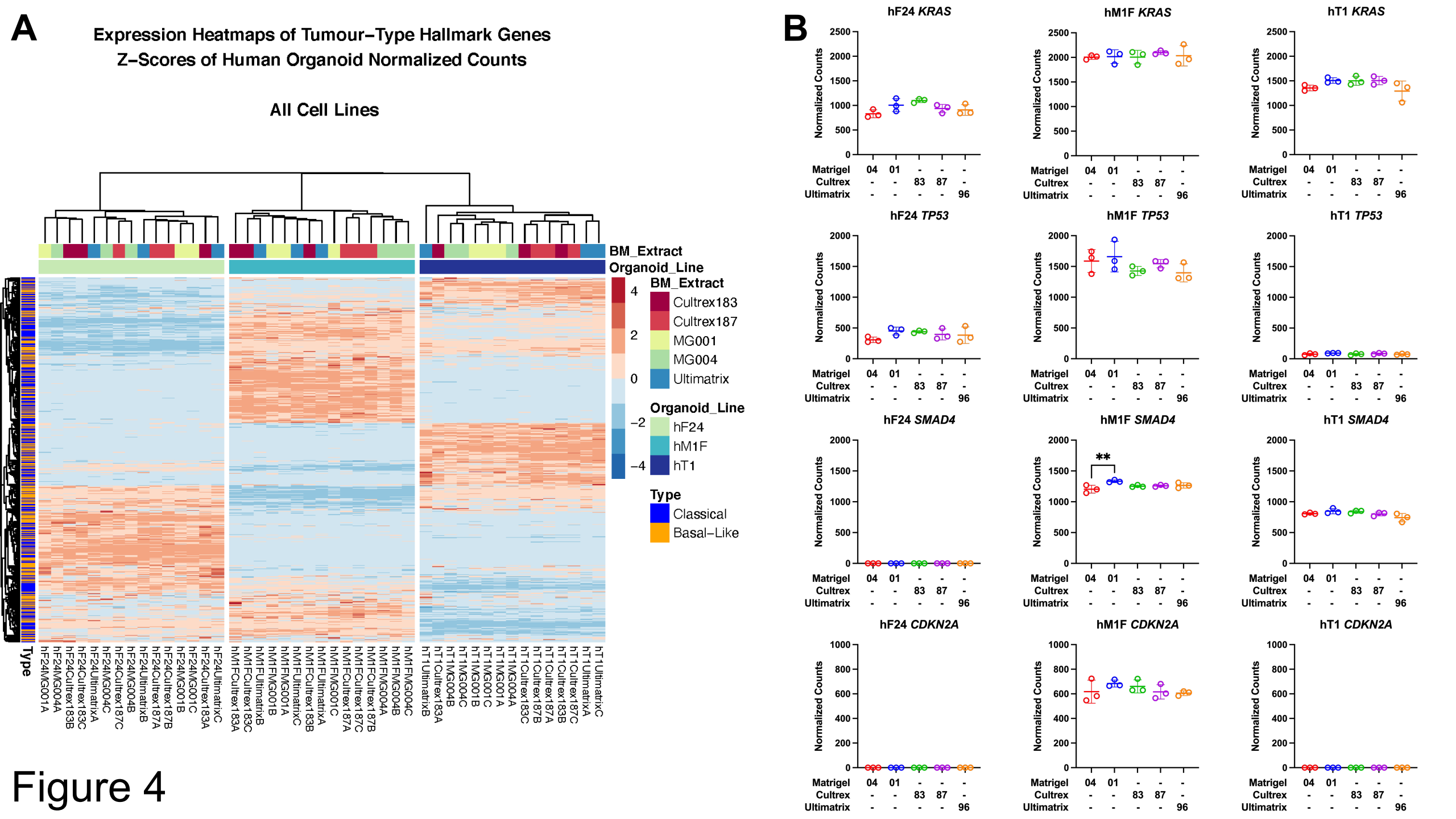
A
Expression Heatmaps of Tumour–Type Hallmark Genes
Z–Scores of Human Organoid Normalized Counts
All Cell Lines
BM_Extract
Organoid_Line
Type
BM_Extract
Cultrex183
Cultrex187
MG001
MG004
Ultimatrix
Organoid_Line
hF24
hM1F
hT1
Type
Classical
Basal–Like
B
hF24 KRAS
hM1F KRAS
hT1 KRAS
hF24 TP53
hM1F TP53
hT1 TP53
hF24 SMAD4
hM1F SMAD4
hT1 SMAD4
hF24 CDKN2A
hM1F CDKN2A
hT1 CDKN2A
Normalized Counts
Matrigel
Cultrex
Ultimatrix
**

Figure 4

Supplementary Figure 1

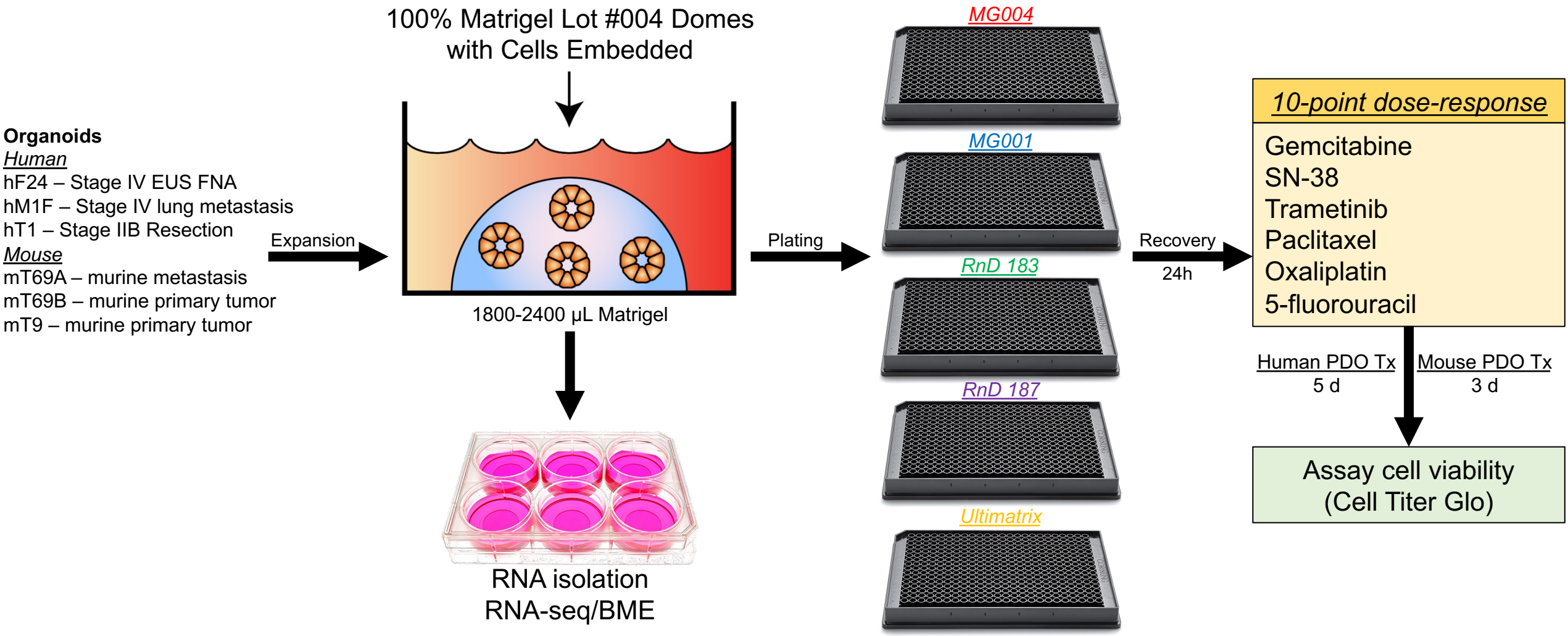

Supplementary Table 1

PDO	Origin	Site	Type of sample	Sex	Age	Race	Stage	KRAS (allele frequencies)	TP53 (allele frequencies)	SMAD4 (allele frequencies)	CDKN2A (allele frequencies)
hF24	H. sapiens	Pancreas	EUS FNA	F	57	Caucasian	4	G12V 82%	F113V (100%)	LOSS (N/A)	DEEP LOSS (N/A)
hM1F	H. sapiens	Lung	RAP	M	55	Caucasian	4	G12D 73%	R175H (100%)	WT (N/A)	WT (N/A)
hT1	H. sapiens	Pancreas	Resection	M	65	Caucasian	2B	G12V 39%	R213* (100%)	WT (N/A)	DEEP LOSS (N/A)

Supplementary Table 2

PDO	Origin	Sex	Site	Type of sample
mT69A	M. musculus	F	Pancreas	KPC B6, PDAC local pancreatic metastasis
mT69B	M. musculus	F	Pancreas	KPC B6, PDAC primary tumor
mT9	M. musculus	F	Pancreas	KPC PDAC primary tumor

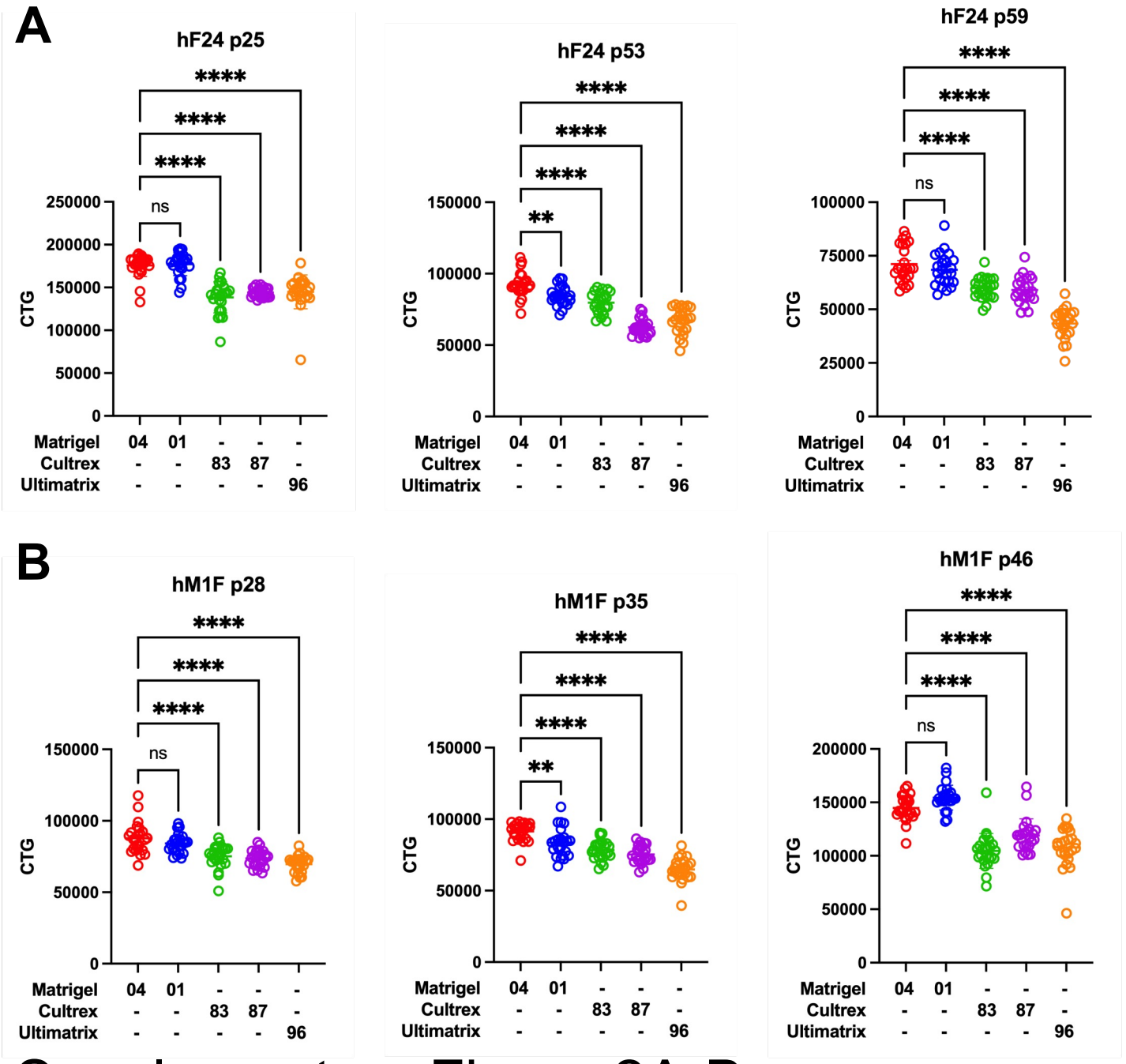

Supplementary Figure 2A-B

C

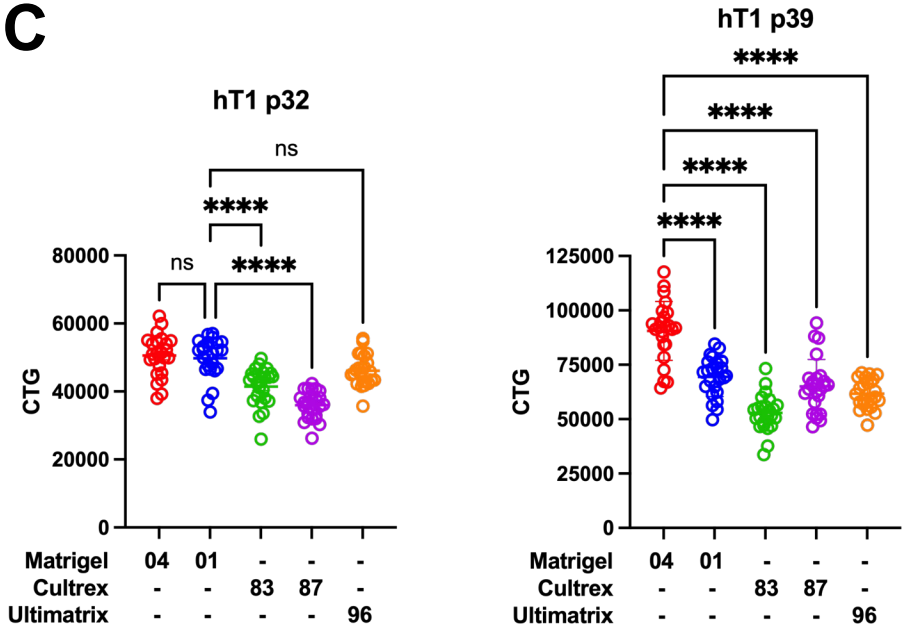

Supplementary Figure 2C

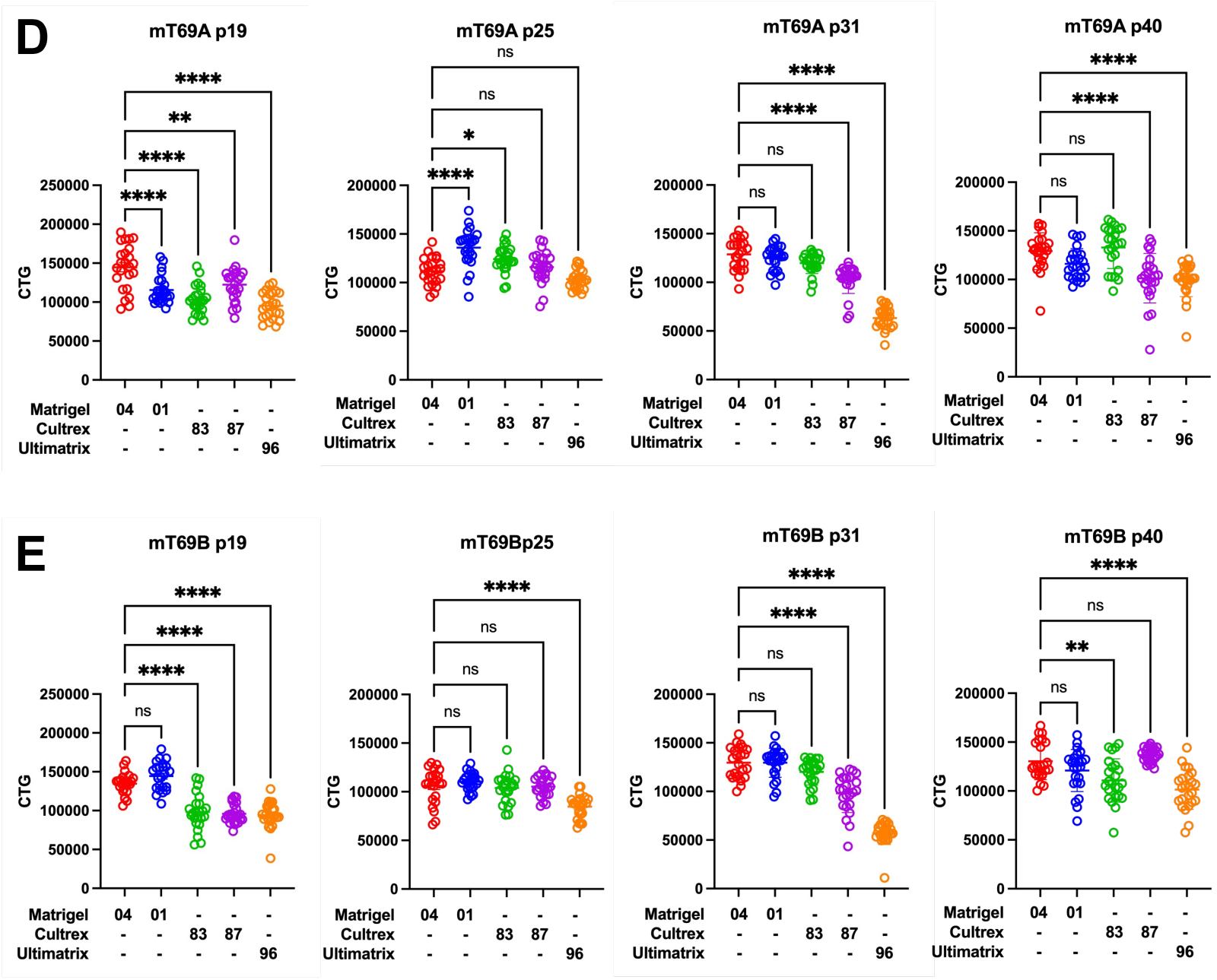

Supplementary Figure 2D-E

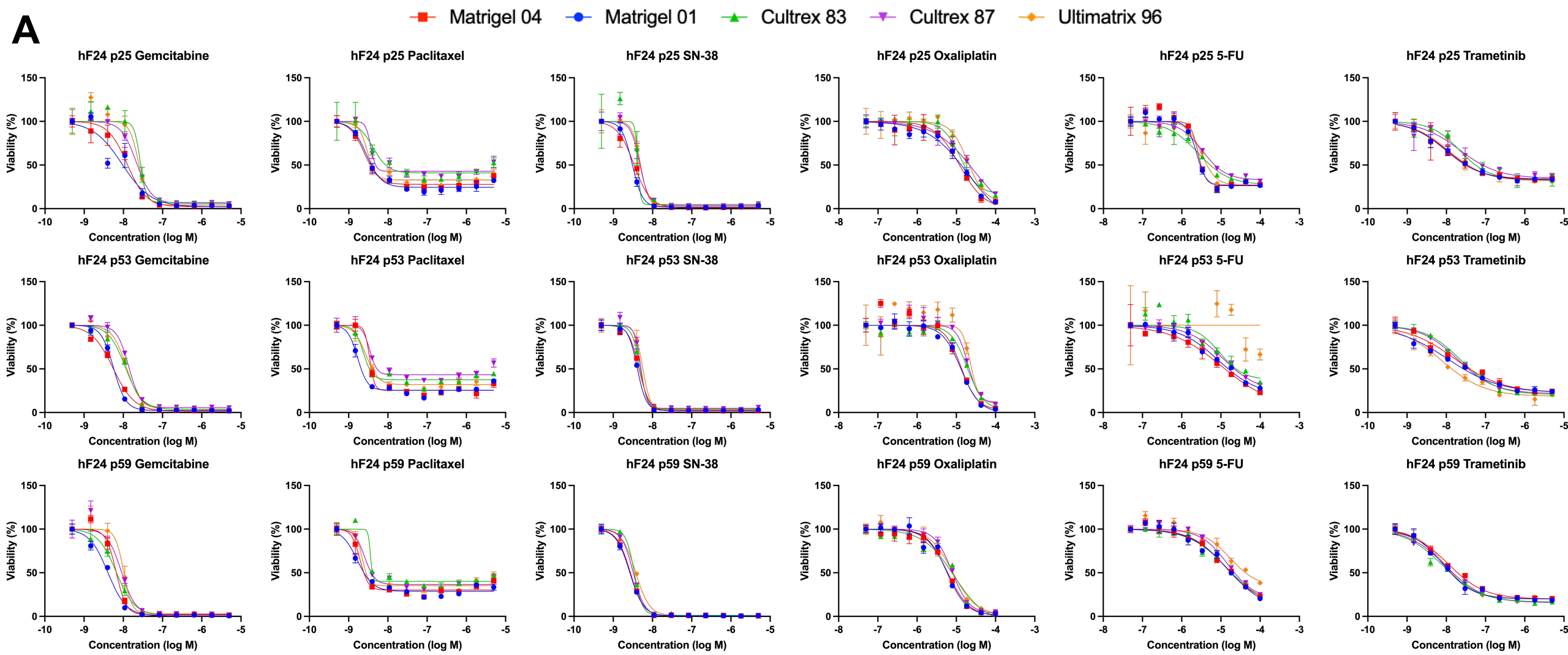

Supplementary Figure 3A

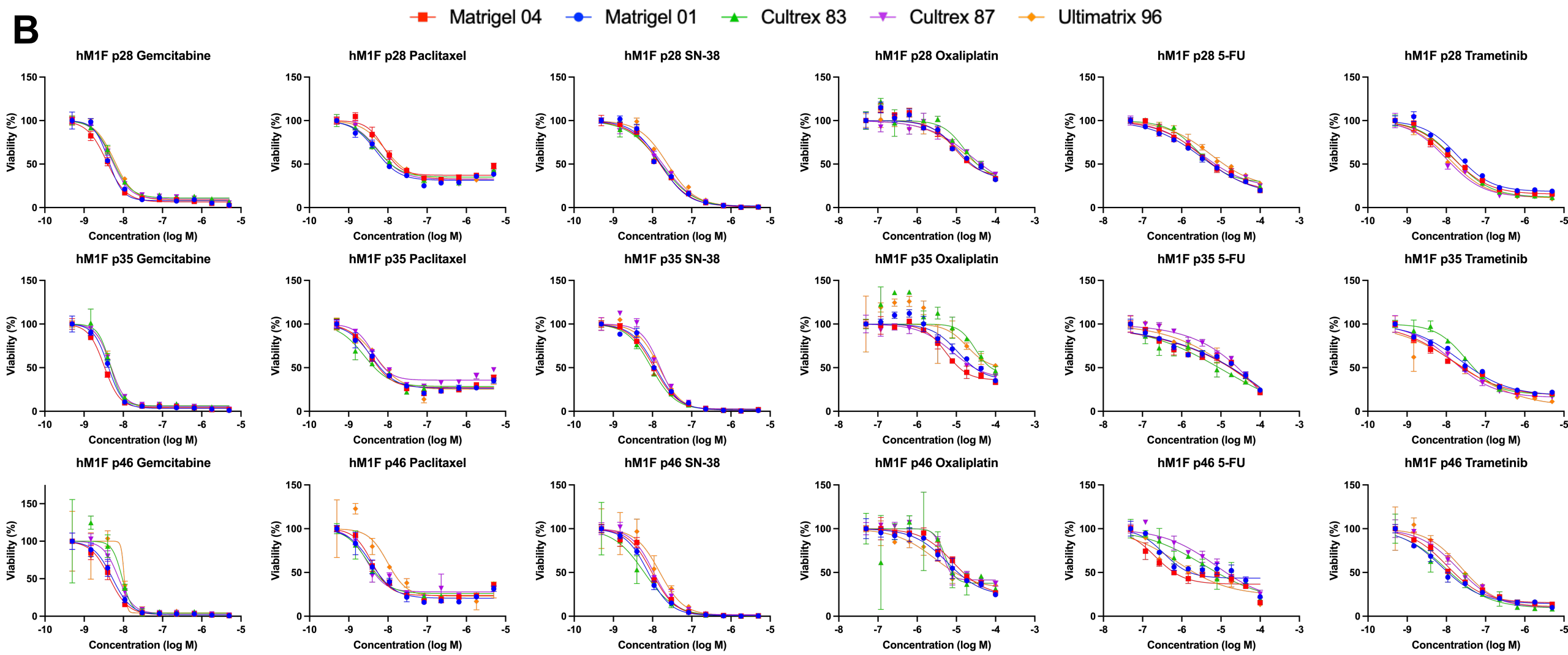

Supplementary Figure 3B

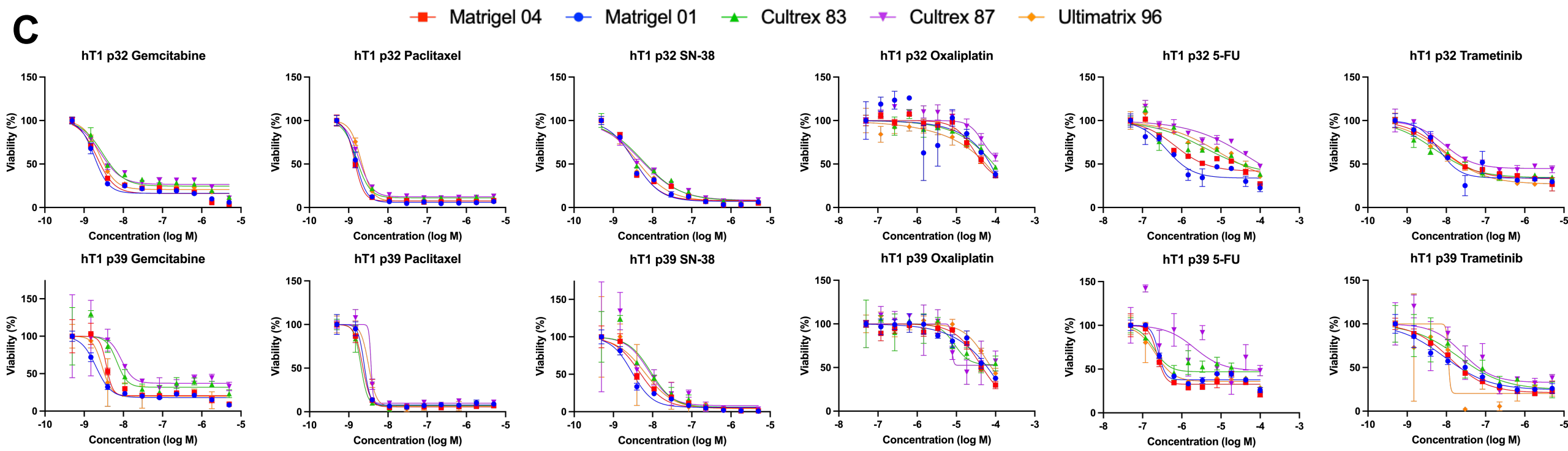

Supplementary Figure 3C

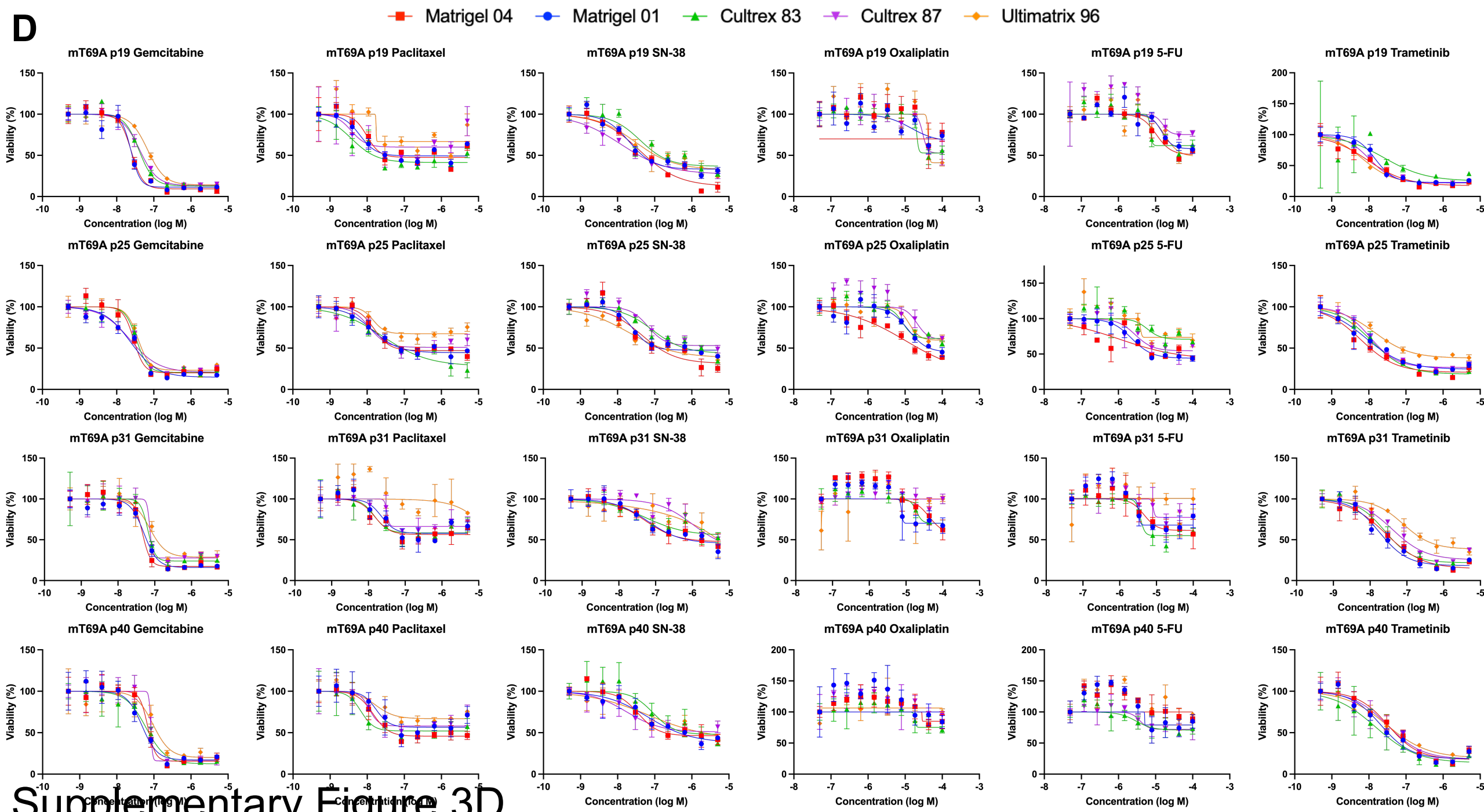

Supplementary Figure 3D

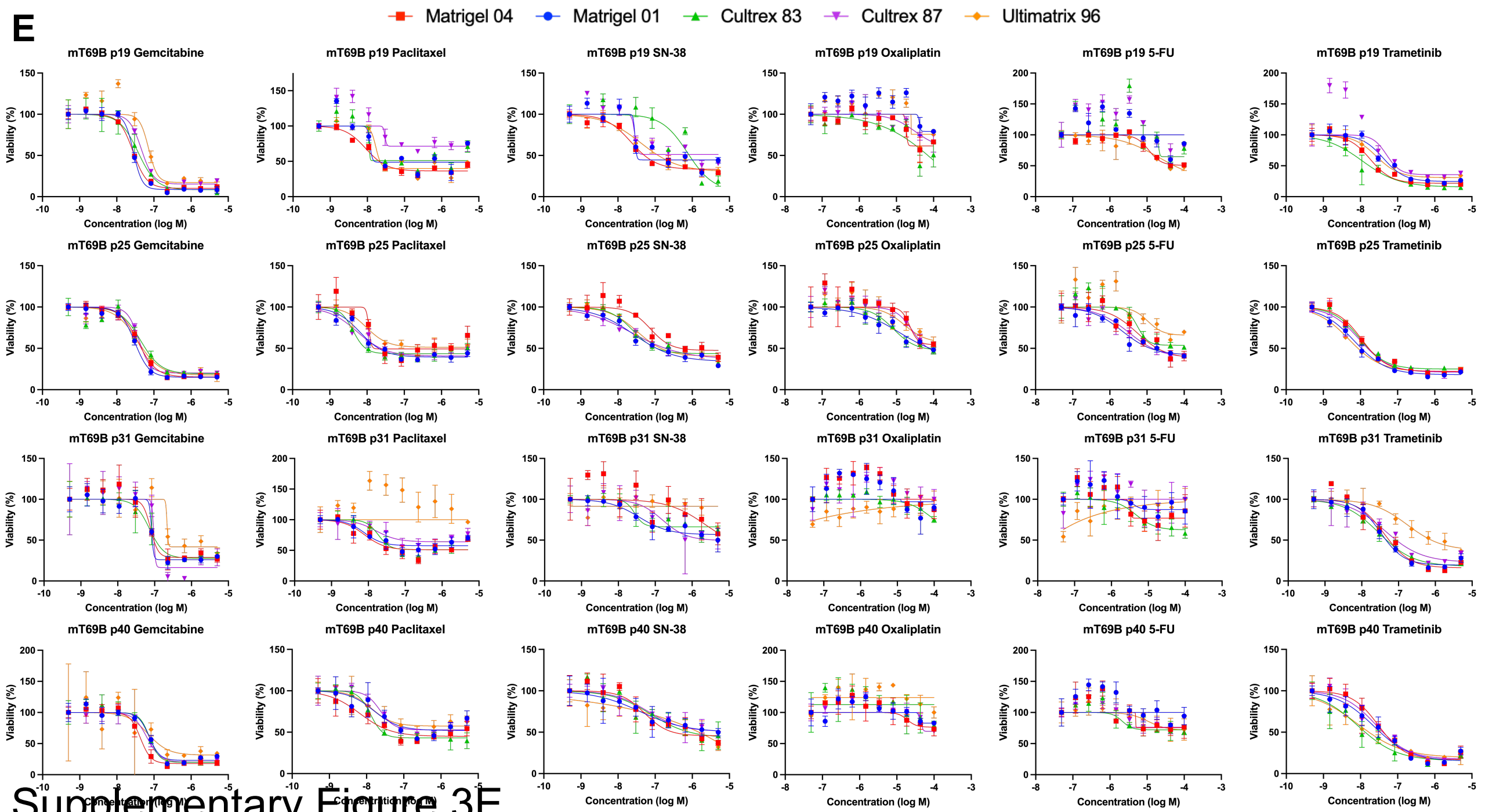

Supplementary Figure 3E

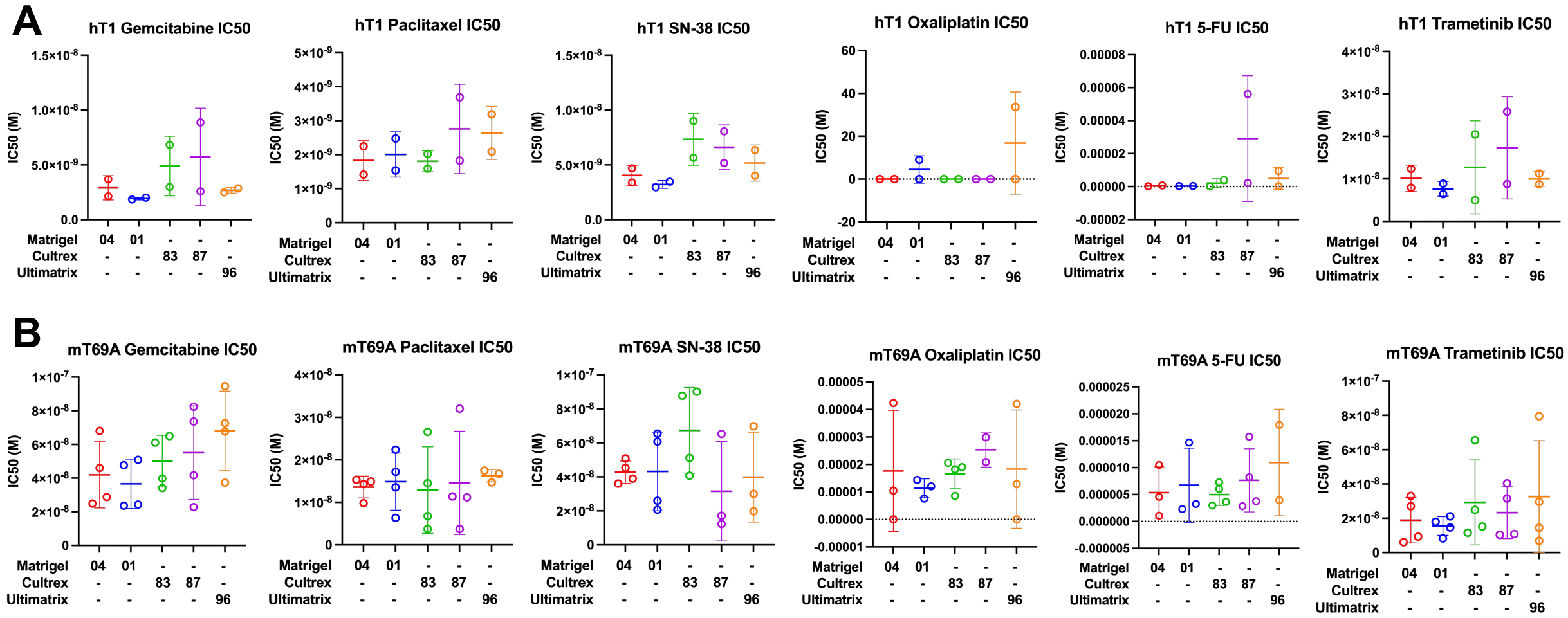

Supplementary Figure 4A-B

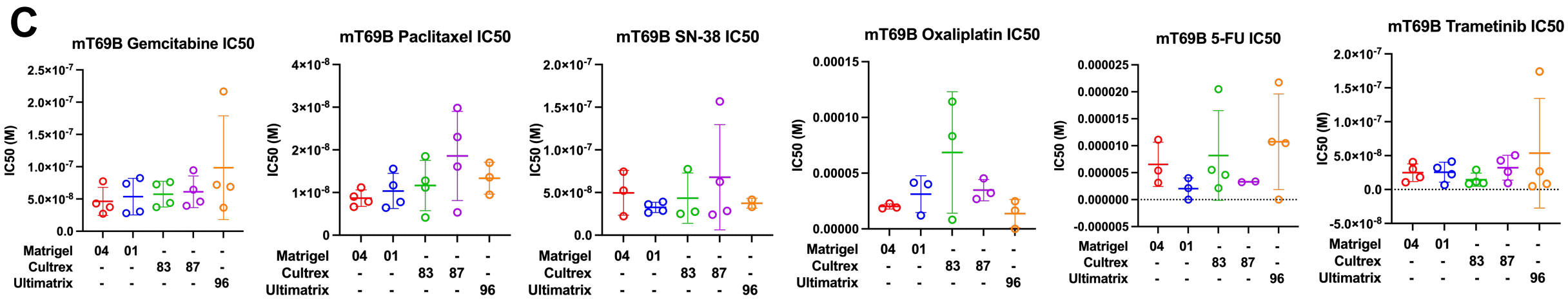

Supplementary Figure 4C

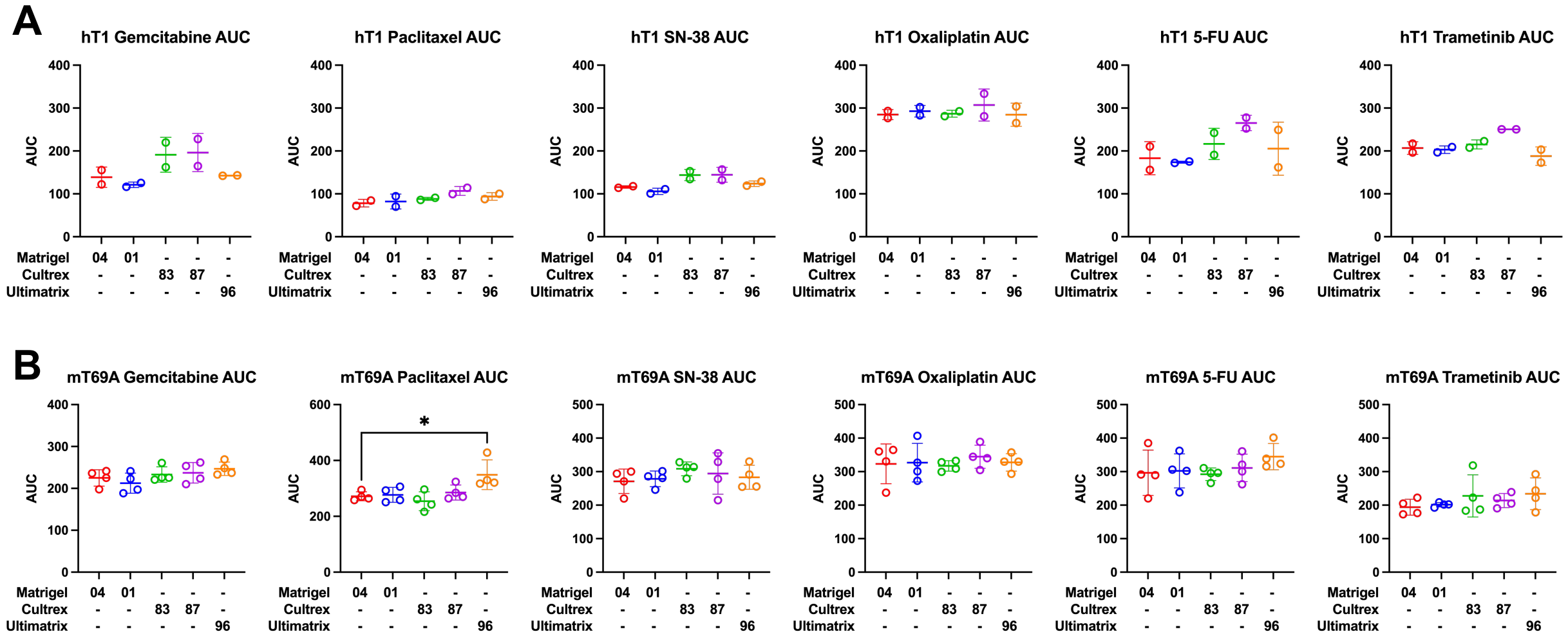

Supplementary Figure 5A-B

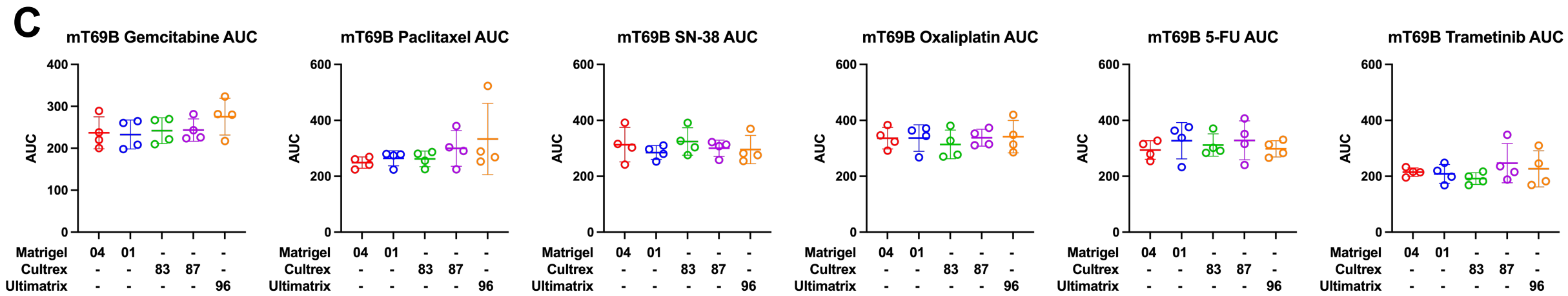

Supplementary Figure 5C

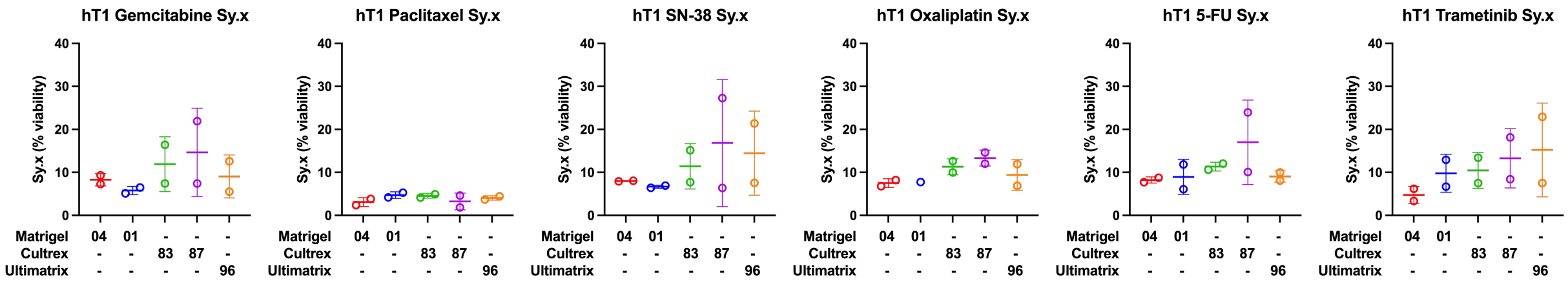

Supplementary Figure 6

A

Total DE Genes Between Basement Membrane Extracts, Humans

Human Samples - All

	Cultrex183	Cultrex187	MG001	MG004	Ultimatrix
Cultrex183	0				
Cultrex187	0	0			
MG001	3	4	0		
MG004	0	50	0	0	
Ultimatrix	0	2	2	70	0

Human Samples - hF24

	Cultrex183	Cultrex187	MG001	MG004	Ultimatrix
Cultrex183	0				
Cultrex187	0	0			
MG001	9	1	0		
MG004	4	0	0	0	
Ultimatrix	0	0	1	0	0

Human Samples - hM1F

	Cultrex183	Cultrex187	MG001	MG004	Ultimatrix
Cultrex183	0				
Cultrex187	2	0			
MG001	0	144	0		
MG004	0	0	20	0	
Ultimatrix	0	6	0	0	0

Human Samples - hT1

	Cultrex183	Cultrex187	MG001	MG004	Ultimatrix
Cultrex183	0				
Cultrex187	4	0			
MG001	5	14	0		
MG004	2	373	2	0	
Ultimatrix	53	14	49	522	0

Cultrex183 Cultrex187 MG001 MG004 Ultimatrix

500 100 10 1

Cells labeled by #DEG (abs(lfc)>1 and FDR≤0.05)

B

Total DE Genes Between Basement Membrane Extracts, Mouse

Mouse Samples - All

	Cultrex183	Cultrex187	MG001	MG004	Ultimatrix
Cultrex183	0				
Cultrex187	0	0			
MG001	9	36	0		
MG004	44	44	0	0	
Ultimatrix	2	34	11	51	0

Mouse Samples - mT69A

	Cultrex183	Cultrex187	MG001	MG004	Ultimatrix
Cultrex183	0				
Cultrex187	0	0			
MG001	3	13	0		
MG004	9	13	1	0	
Ultimatrix	0	18	12	23	0

Mouse Samples - mT69B

	Cultrex183	Cultrex187	MG001	MG004	Ultimatrix
Cultrex183	0				
Cultrex187	0	0			
MG001	47	88	0		
MG004	58	90	1	0	
Ultimatrix	4	10	61	77	0

Mouse Samples - mT9

	Cultrex183	Cultrex187	MG001	MG004	Ultimatrix
Cultrex183	0				
Cultrex187	0	0			
MG001	4	6	0		
MG004	11	15	0	0	
Ultimatrix	6	14	5	12	0

Cultrex183 Cultrex187 MG001 MG004 Ultimatrix

500 100 10 1

Cells labeled by #DEG (abs(lfc)>1 and FDR≤0.05)

Supplementary Figure 7A-B

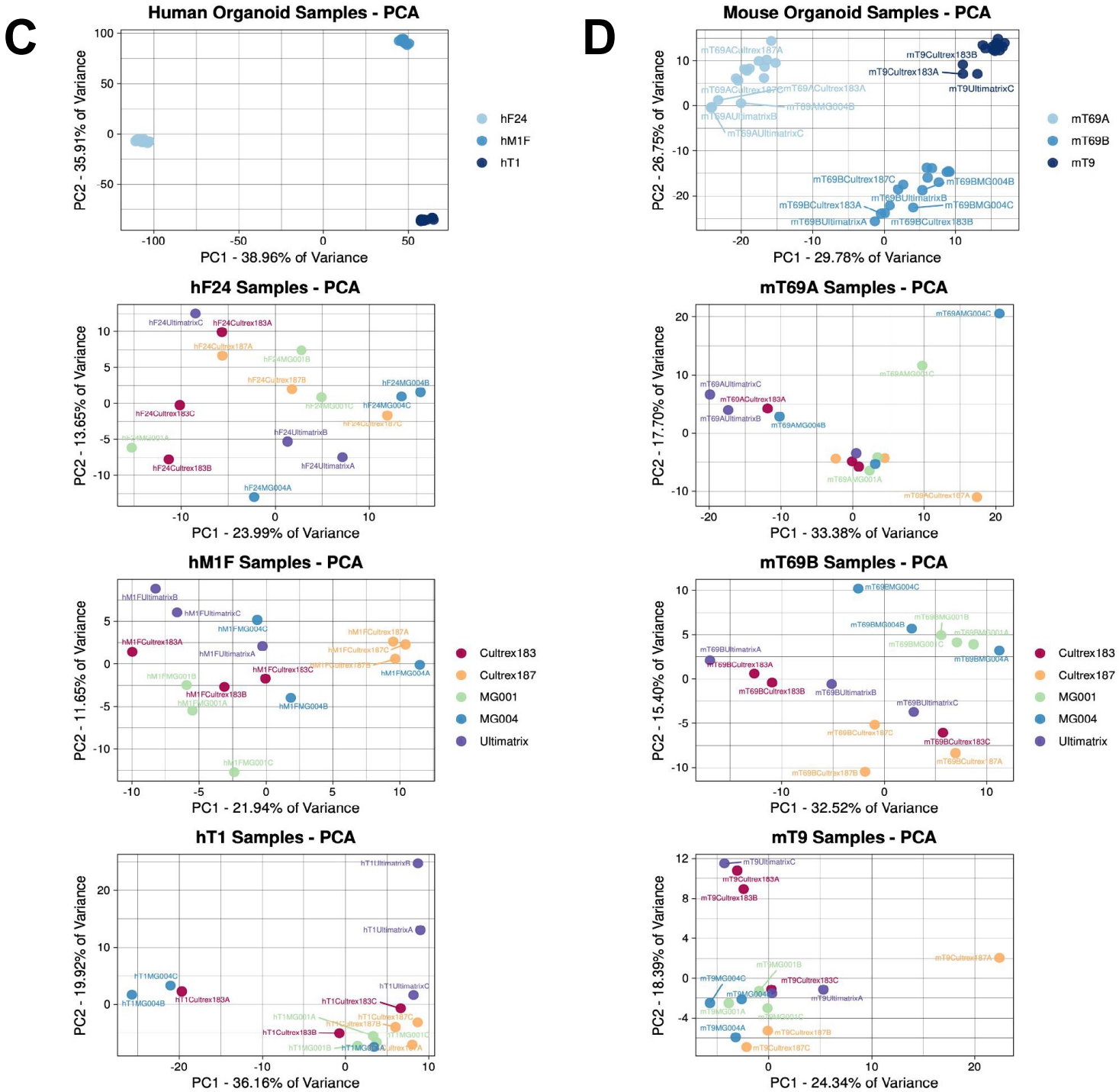

Supplementary Figure 7C-D

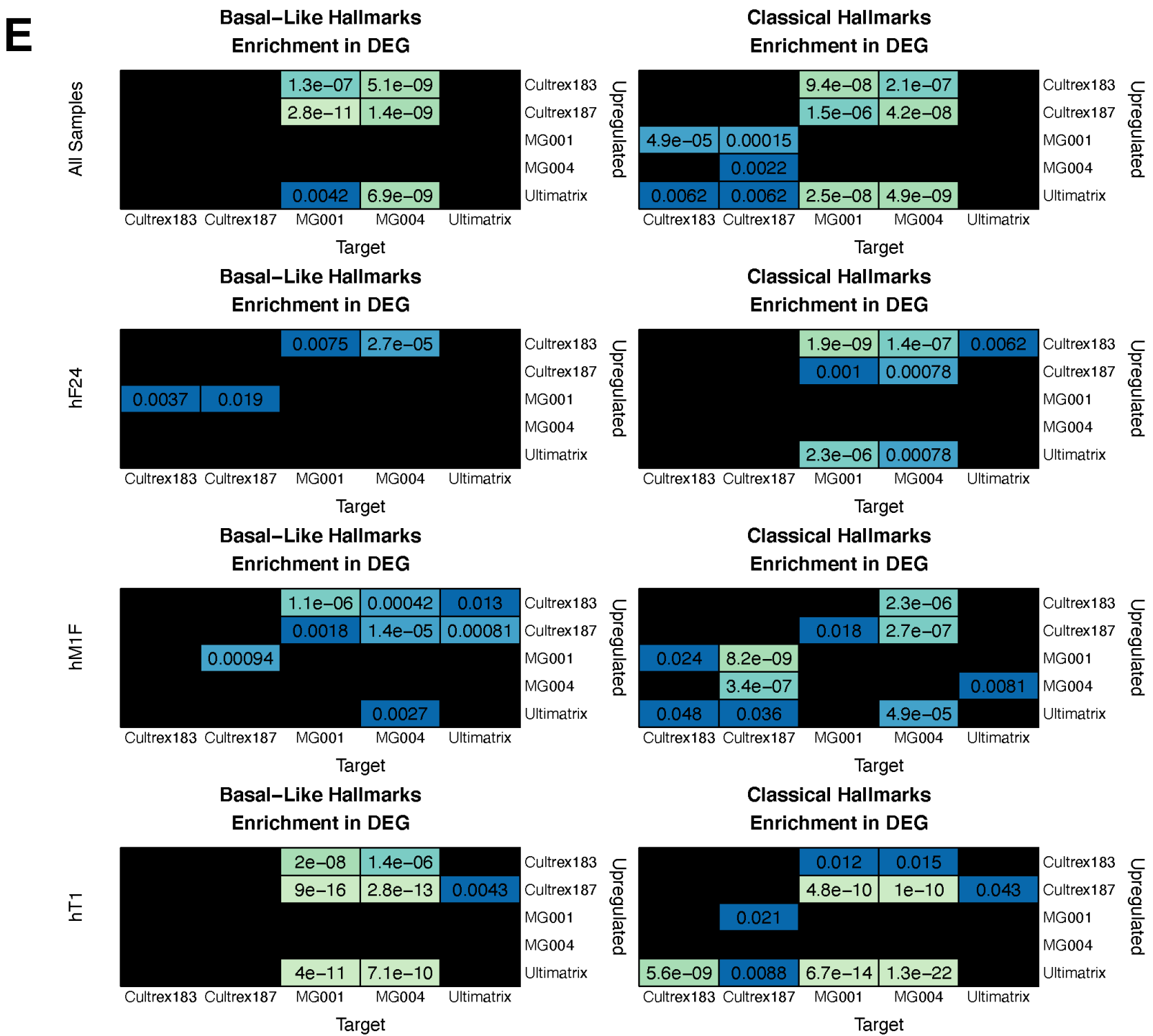

Supplementary Figure 7E

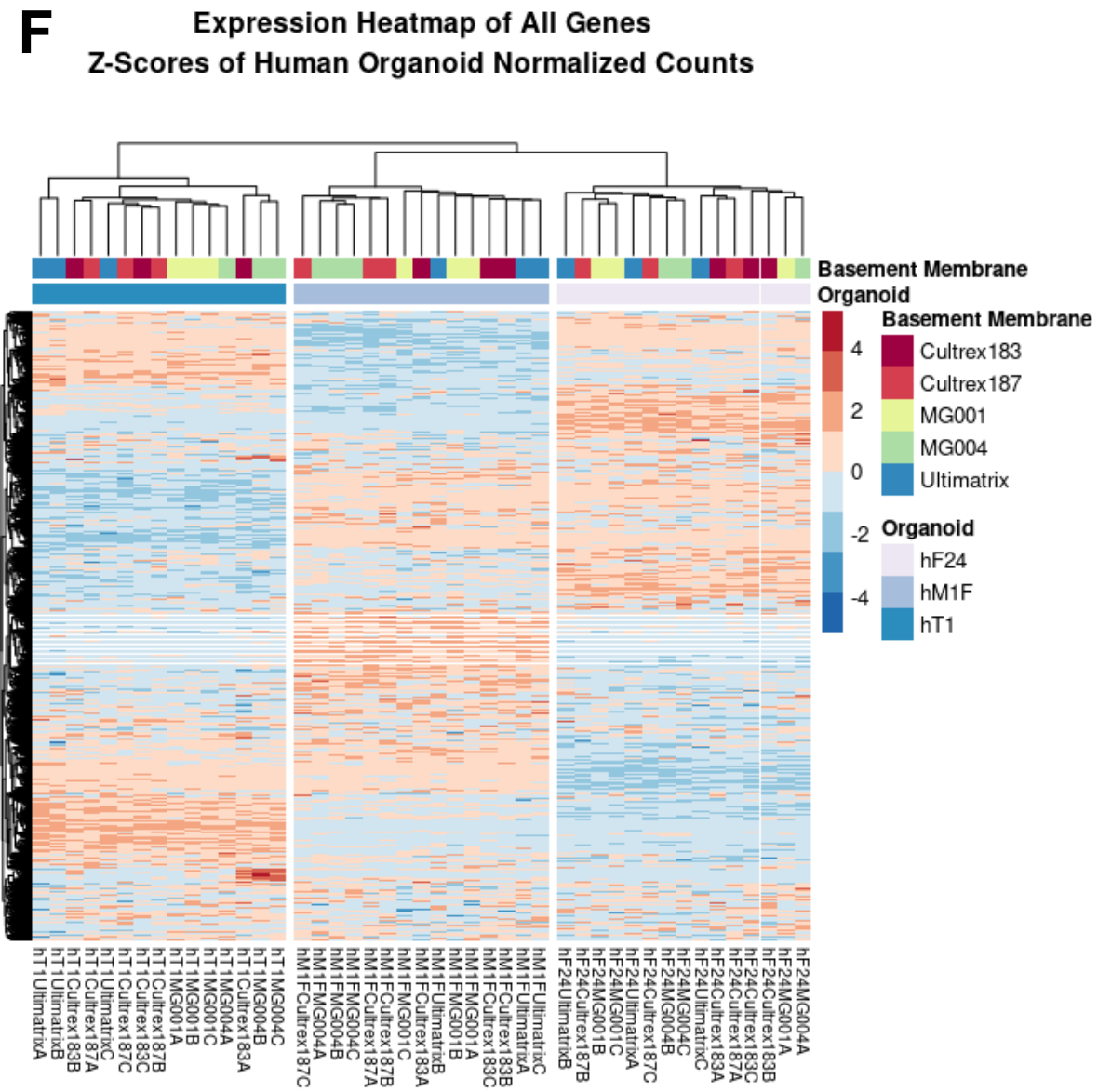

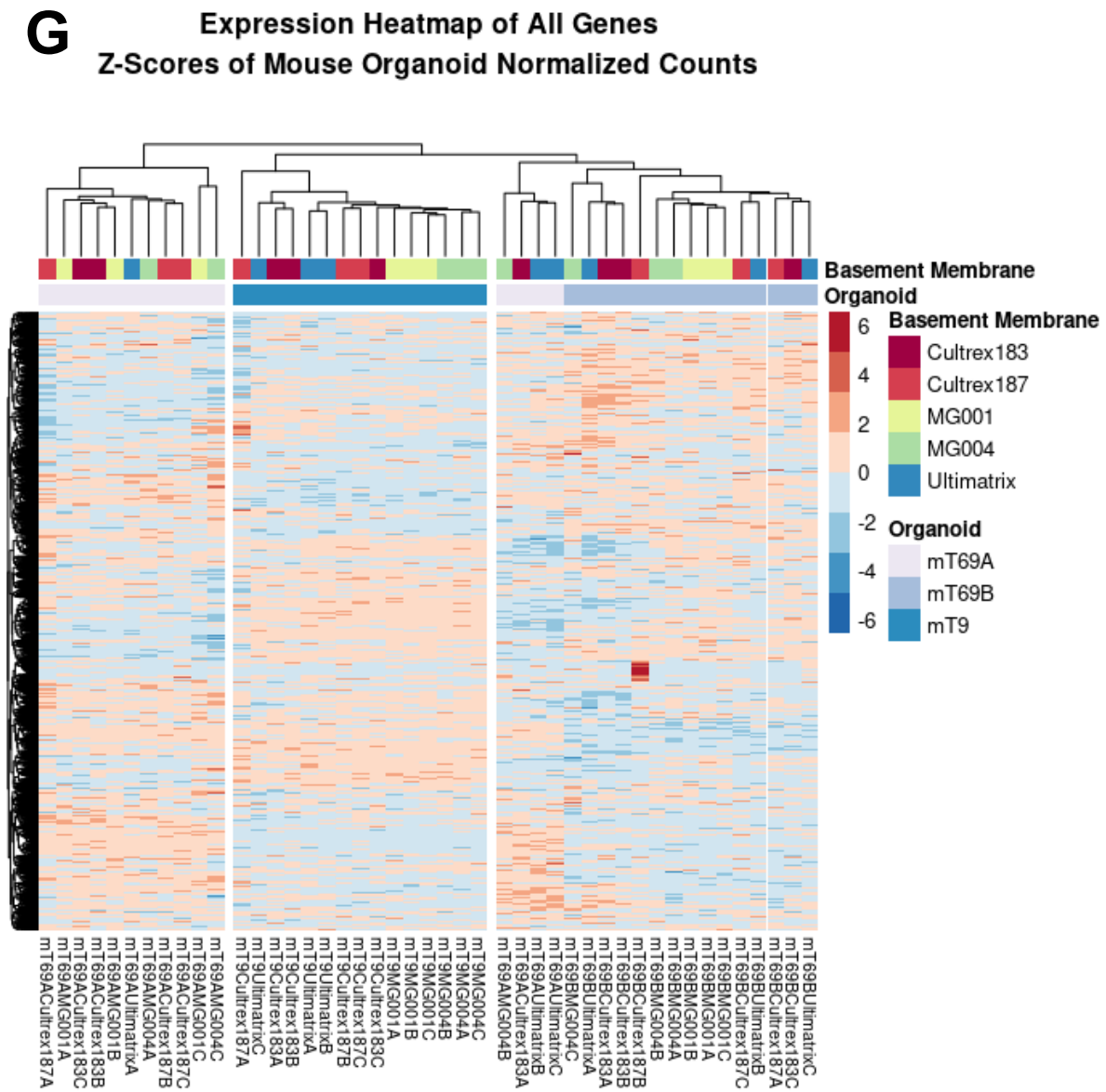

Supplementary Figure 7F-G

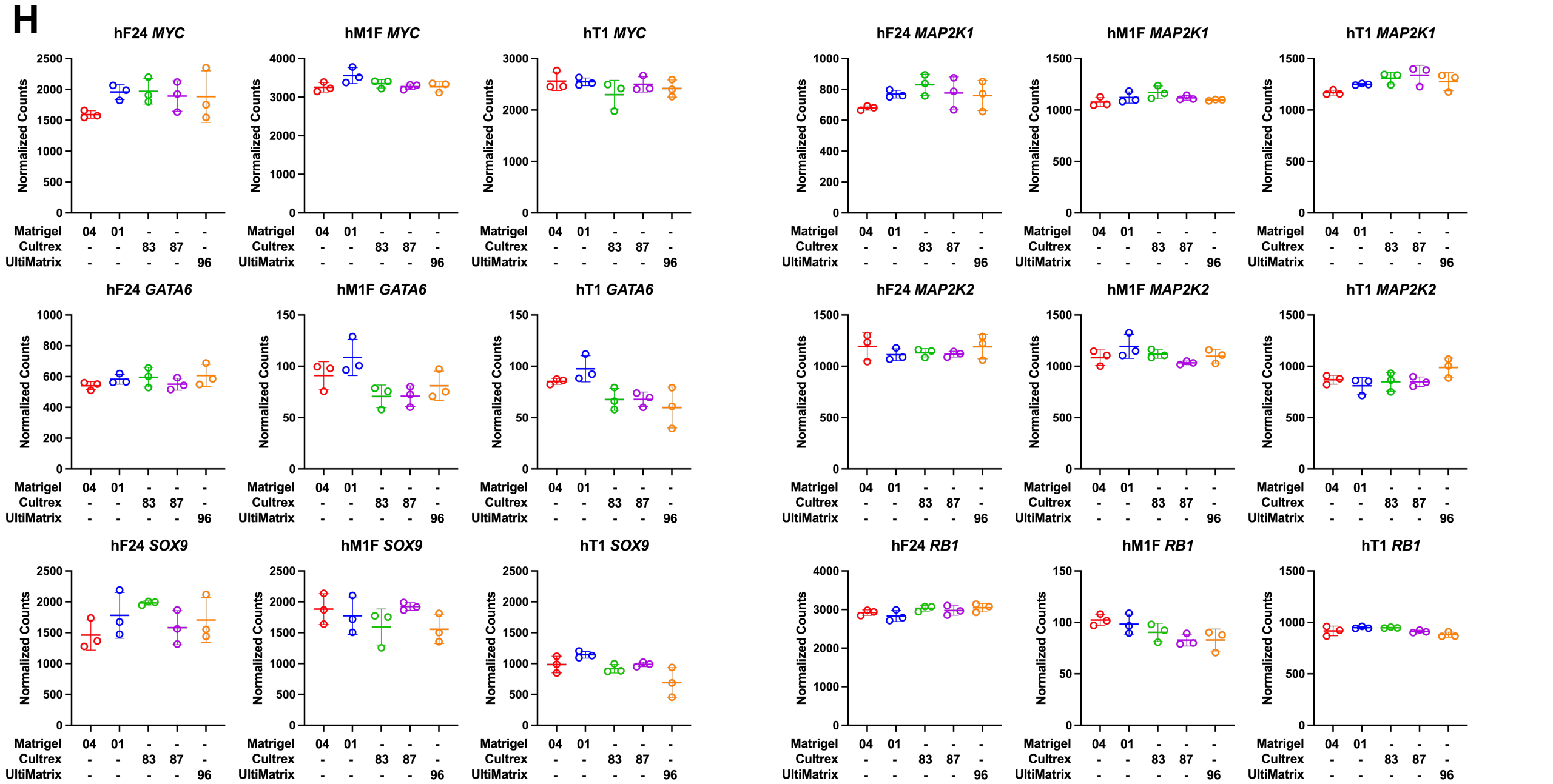

Supplementary Figure 7H

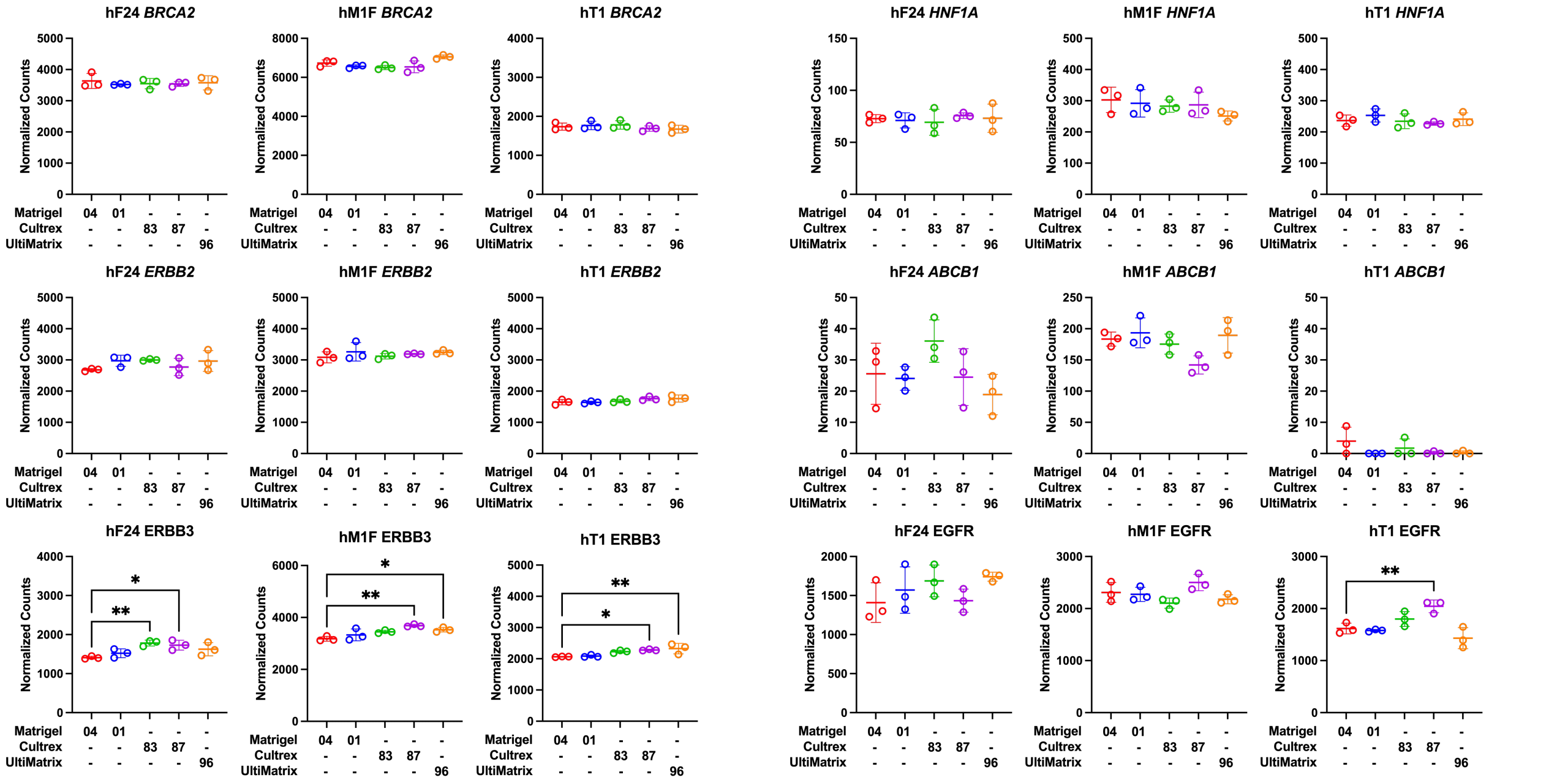

Supplementary Figure 7H